Copyright Warning & Restrictions

The copyright law of the United States (Title 17, United States Code) governs the making of photocopies or other reproductions of copyrighted material.

Under certain conditions specified in the law, libraries and archives are authorized to furnish a photocopy or other reproduction. One of these specified conditions is that the photocopy or reproduction is not to be "used for any purpose other than private study, scholarship, or research." If a, user makes a request for, or later uses, a photocopy or reproduction for purposes in excess of "fair use" that user may be liable for copyright infringement,

This institution reserves the right to refuse to accept a copying order if, in its judgment, fulfillment of the order would involve violation of copyright law.

Please Note: The author retains the copyright while the New Jersey Institute of Technology reserves the right to distribute this thesis or dissertation

Printing note: If you do not wish to print this page, then select "Pages from: first page # to: last page #" on the print dialog screen

ABSTRACT

Photoluminescence Study of Gallium Arsenide, Aluminum Gallium Arsenide, and Gallium Antimonide Thin Films Grown by Metalorganic Chemical Vapor Deposition

by
John Mark Koons

The photoluminescence produced by four MOCVD grown epitaxial thin film samples was studied to give insight into sample quality. The four samples under this study were GaAs on a GaAs substrate, $Al_{.25}Ga_{.75}As$ on a GaAs substrate, $Al_{.30}Ga_{.70}As$ on a GaAs substrate, and GaSb on a GaSb substrate. Excitation was achieved through the use of the 514.0 nm line of an argon ion laser, and sample cooling was attained by use of a cryostat cooler using helium gas to attain a low temperature limit of 10°K. The GaAs and $Al_{.30}Ga_{.70}As$ samples exhibited typical spectra for MOCVD grown samples produced by other sources in the widths of the resulting BE peaks and in the characterisitics of their acceptor-induced transitions. The narrow, prominent BE peaks of the $Al_{.25}Ga_{.75}As$ and GaSb samples had shown them to be of exceptional quality.

PHOTOLUMINESCENCE STUDY OF GALLIUM ARSENIDE, ALUMINUM GALLIUM ARSENIDE, AND GALLIUM ANTIMONIDE THIN FILMS GROWN BY METALORGANIC CHEMICAL VAPOR DEPOSITION

by
John Mark Koons

A Thesis
Submitted to the Faculty of
New Jersey Institute of Technology
in Partial Fulfillment of the Requirements for the Degree of
Master of Science in Applied Physics

Department of Physics

January 1994

APPROVAL PAGE

PHOTOLUMINESCENCE STUDY OF GALLIUM ARSENIDE, ALUMINUM GALLIUM ARSENIDE, AND GALLIUM ANTIMONIDE THIN FILMS GROWN BY METALORGANIC CHEMICAL VAPOR DEPOSITION

John Mark Koons

Dr. K. Ken Chin, Thesis Advisor — Date
Professor of Physics, NJIT

Dr. John G. Hensel, Committee Member — Date
Distinguished Research Professor of Physics, NJIT

Dr. Halina Opyrchal, Committee Member — Date
Visiting Professor of Physics, NJIT

BIOGRAPHICAL SKETCH

Author: John Mark Koons

Degree: Master of Science in Applied Physics

Date: January 1994

Undergraduate and Graduate Education:

- Master of Science in Applied Physics,
  New Jersey Institute of Technology, Newark, NJ, 1994

- Bachelor of Arts in Physics,
  Rutgers College, New Brunswick, NJ, 1991

Major: Applied Physics

ACKNOWLEDGMENT

The author would like to express gratitude to his advisor, Professor K. Ken Chin, for his support in this work and throughout the entire graduate experience.

A special appreciation for time and effort spent by Dr. Halina Opyrchal in this study is to be noted, for providing a great deal of help with all aspects of this study.

The author also thanks Professor Yuan Yan for his suggestions and Professor John C. Hensel for his valuable input and donation of much of the laboratory equipment used.

TABLE OF CONTENTS

TABLE OF CONTENTS
(Continued)

LIST OF TABLES

Table **Page**

LIST OF FIGURES

Figure **Page**

CHAPTER 1

THIN FILM TECHNOLOGY FOR OPTOELETRONICS

1.1 Introduction

Advancements in the development of state of the art semiconductor optoelectronic devices such as lasers, photodetectors, and modulators hinge upon the technologies needed to create high quality thin films which are necessary in device production. The precise control over impurity distributions and lattice defects necessary to produce optimal performance for these devices is due to research efforts made by materials scientists. Several methods of thin film production are currently used, each one having a unique set of growth conditions, expected film quality, and set of production costs associated with it. Three common growth methods are vapor-phase epitaxy (VPE), liquid-phase epitaxy (LPE), and molecular beam epitaxy (MBE). Their names indicate the phase of the material from which the desired film is constructed by a deposition process.

It is a common practice to deposit III-V compound semiconductor thin film layers on a substrate of the same bulk material that has been grown by another process which provides for large single crystal formation. The resulting film may be tailored to give a bandgap of desired energy when a compound of three semiconductors (ternary compound) is formed by varying the compositional ratios. The films in this study were all developed by a specific type of vapor-phase epitaxy called metalorganic chemical-vapor deposition (MOCVD). Therefore this process will be discussed briefly to give some insight into the quality of the single crystal film or alloy and expected unintentional impurities, both of which will govern its light-emitting properties. Although all samples were grown by MOCVD in this study, a discussion of the MBE process will follow this since it is a favored technique for producing heterostructures of very thin, rapidly alternating layers.

1.2 MOCVD Process

Thin film production by the MOCVD process is a specialized case of vapor-phase epitaxy which derives its name from the gases used for crystal formation. In III-V compounds, such as gallium arsenide, the metallic element (gallium) is introduced through a trimethyl compound gas, which would be trimethylgallium in this case ($(CH_3)_3Ga$). One incentive for using this method is in the reduced toxicity of the process gases involved as compared to using standard VPE growth. The process involves introducing the appropriate gases into a reaction chamber holding a substrate that acts as a seed upon which the film will grow by deposition. Since the growing film will replicate the pattern of the seed, the substrate is typically a wafer of material which has a crystal structure and lattice constant desirable for the film to possess. The reaction takes place near 700°C, so the wafer is heated by conduction through a sample holder, and may be rotated in some cases to provide for more uniform growth. Therefore, control over the growth process may be achieved by changing the gas flow rates, absolute pressure within the chamber, the sample temperature, and/or the rotation rate for the holder. Studies have been conducted which show that increasing rotational speed, decreasing reaction temperature, and increasing Ga to As flux ratios will tend to form more defect-free layers (Swaminathan, Van Haren, Zilko, Lu, and Schumaker 1985, 5353). The reaction describing thin film growth of gallium arsenide is

$$(CH_3)_3Ga + AsH_3 \rightarrow GaAs + 3CH_4\uparrow$$

while the growth of AlGaAs can be achieved by simply adding trimethylaluminum gas ($(CH_3)_3Al$). It may be possible to dope the growing crystal by adding impurities during the reaction to produce a controlled density of donor and/or acceptor atoms that will determine its electrical and optical properties. By varying the gas composition during the growth, alternating layers of GaAs and AlGaAs may be obtained, which are necessary in semiconductor laser heterostructure fabrication.

1.3 MBE Process

Thin film growth by MBE can be characterized as having the best control over thin layer deposition, although requiring the most sophisticated equipment as well. For this process, a sample is contained in vacuum at a controlled temperature (about 600 to 650°C for GaAs formation) while beams of molecules or atoms of the growth layer components are directed at its surface. Components are heated in separate crucibles, each of which have exits for the molecular or atomic beam. The individual beams may be controlled by shutters in front of the crucibles that can open or close at varying intervals, which would allow for alternating layers to be produced. Since the layers can be controlled in this way to produce variations down to the order of a single monolayer, the technique allows for easy production of heterostructures and strained layer epitaxial growth. In the latter, a film is grown onto a substrate whose lattice constant does not match the one for the deposited layer. Crystal defects can be minimized by forming thin alternating layers that gradually relieve any surface strains causing the defects.

CHAPTER 2

THEORY OF PHOTOLUMINESCENCE IN DIRECT-GAP SEMICONDUCTORS

2.1 Photoluminescence as a Characterizational Tool

A direct-gap semiconductor will have both electrical and optical properties of interest which need to be characterized by experimental methods. Electrical properties such as carrier concentration and mobility may be determined through conductivity and Hall coefficient measurements. Material properties such as photoemission efficiency, carrier lifetimes, band gap size, impurity concentrations, and defect densities may be determined through several techniques such as absorption coefficient measurements, photoconductive decay experiments, and luminescence measurements.

The role of photoluminescence characterization is to provide a means for a non-destructive process to be performed on samples that give insight to some of its material properties listed above. Primarily, photoluminescence experiments have the potential for providing a map of major impurities within a given sample and giving insight to the crystal quality when used to examine a single crystal sample. They have an advantage over any chemical analysis process in this area, which may be prohibitive due to high cost or due to the trace amounts of substances being examined within a sample. A careful set of experiments performed with variation of experimental parameters such as sample temperature can provide for identification of low concentration impurities as well as possibly giving some other optical parameters of interest. For an alloy (a ternary or quaternary semiconductor), one the most important uses of photoluminescence lies in bandgap determination of the compound.

2.2 Introduction to the Photoluminescence Process

All luminescent processes must first involve the excitation of carriers from lower to higher energy states. Once in these higher states, they may decay to lower states by giving up heat to the lattice and/or emitting photons of a given energy. This excitation process typically moves electrons from the valence band to the conduction band to generate an electron-hole pair, and may be achieved through several methods.

The three common types of excitation are cathodoluminescence (using electron bombardment), electroluminescence (use of current injection), and photoluminescence (use of a light source). The first type of luminescence forms the basis for cathode ray tube operation, in which high energy electrons strike a phosphorus coating to produce an image. The second type is widely utilized in photonic devices, including light emitting diodes (LEDs) and lasers. The third occurs in all fluorescent lamps, where UV and near UV light produced by a gas source is converted to longer wavelength light over a broad range by the phosphorous coating on the lamp.

In the research field, photoluminescence is achieved by the use of a powerful light source, such as a laser, which will provide photons of an energy equal to or greater than the band gap energy for the semiconductor sample being studied. Using a light source whose photons have an energy of at least the band gap value enables electrons to move into the available states in the conduction band, from which they will decay with a given time constant since they are not at thermal equilibrium with the lattice. In a highly doped semiconductor, the Fermi level may be within the conduction or valence band due to excess donors or acceptors, respectively. In this case, the material is said to be degenerate. A pure or lightly doped sample will have its Fermi level well within the energy gap. This means that when electron-hole pairs are created in numbers that are large compared to the total number of available states, the excess pairs will combine since they are not in a balanced state with the crystal.

When referring to the steady-state excitation of a semiconductor which causes an excess number of carriers to form due to this external perturbation and not from an increase in sample temperature, it is common to use quasi-Fermi levels to show the expected carrier populations for each band. Steady-state excitation, in which a constant flow of photons is provided to the sample, will raise the quasi-Fermi level for electrons and depress this level for holes, so that the continual formation of electron-hole pairs and their expected number at any given time is reflected. In steady-state, the continual formation of carrier pairs means their continual recombination as well, and at the same rate.

2.3 Absorption Mechanisms

2.3.1 Introduction

All materials may be characterized by an absorption coefficient that describes the rate of absorption of light with respect to distance. This coefficient, α, is dependent upon the wavelength of light used and on the material. The intensity of light transmitted through a distance x is then given by

$$I(x) = I_O e^{-\alpha x}$$

Here, I_O is the original light intensity. The absorption coefficient for semiconductors will be negligible for photon energies far below the band gap and increase greatly for energies above the band gap. Photons which possess energies too small to excite electrons into available states in the conduction band will pass through the crystal unaffected, and the crystal will appear transparent to these photons. If the photons do possess at least the minimum energy for excitation processes, the coefficient will reflect the total effect of all processes that may occur for the given photon energies. The total rate of absorption is a summation of all absorption rates, each occurring with a different probability. Therefore, some processes may dominate so others will take place at a negligible rate within a given crystal. The rate of occurrence for any process will vary from one sample to another, so a brief introduction will be provided for all absorption mechanisms.

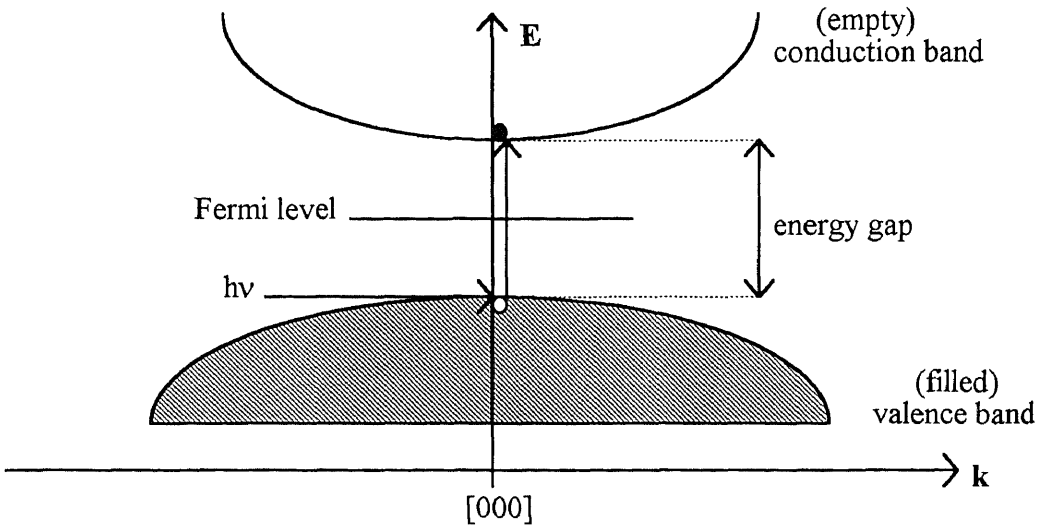

Figure 2.1 Creation of an electron-hole pair by interband transition in a direct-gap semiconductor. The incoming photon possessed an energy equal to the band gap, and the semiconductor was at 0 K prior to the transition.

Photon absorption processes involving charge carriers within semiconductors include interband, exciton, free carrier, and intraband transitions as well as transitions involving impurity states. In discussing each of these processes, it will first be assumed that the crystal is not doped and at 0°K so that all lower energy states are filled and all upper states are empty when no external excitation source is present.

2.3.2 Interband Absorption

Interband absorption involves excitation of an electron from valence band to conduction band. Energy conservation can be applied to this process by writing

$$E_f = h\nu - E_i$$

Initial and final electron energy states are given by E_i and E_f, respectively, and $h\nu$ is the photon energy. Momentum conservation must be applied to this transition as well, and in

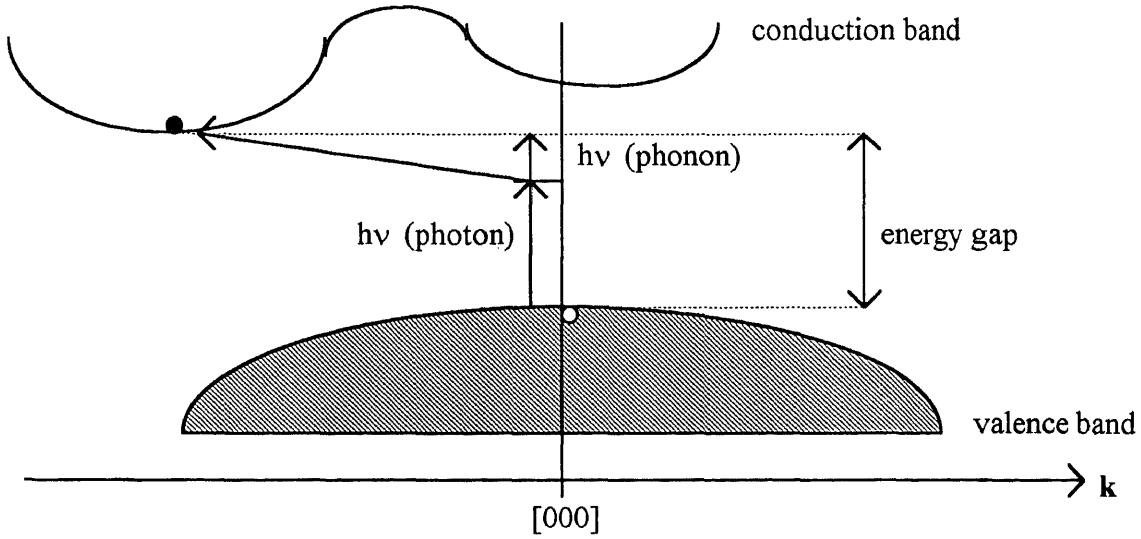

Figure 2.2 Creation of an electron-hole pair by interband transition in an indirect gap semiconductor. Phonon absorption provides the necessary momentum change to complete the transition for the case shown here. Phonon emission requires that the incident photon possess an energy larger than the bandgap.

doing so it becomes apparent that not all energy conserving processes are allowed. The momentum of a photon having a given wavelength λ is

$$p = E/c = h\nu/c = h/\lambda.$$

Likewise, crystal momentum is given by

$$p = h/\lambda_{ph}$$

with λ_{ph} being the phonon wavelength, which has a minimum value of the order of the lattice constant. Since the crystal momentum is typically much larger than the photon momentum, the latter can usually be neglected.

A plot of electron and hole energy versus momentum within the crystal can be seen in an E-k diagram, which is a valuable tool for solid state analysis. In the diagram, the wavevector k represents momentum;

$$k = 2\pi p/h$$

A transition that conserves electron momentum will manifest itself as a vertical upwards line in an E-k diagram, from valence to conduction band. A semiconductor's energy gap is

defined as the minimum distance between the conduction and valence band. If the maximum of the valence band and minimum of the conduction band occur at the same point in k space, the crystal will be a direct gap semiconductor. Indirect gap semiconductors have a band structure in which the minimum distance between valence and conduction bands does not occur at the same point in momentum space. An indirect gap crystal will therefore require photons of an energy larger than the band gap to create electron-hole pairs if no intervening process takes place.

It should be noted that due to quantum mechanical selection rules, absorption (and emission) of photons at $k = 0$ may not be permitted for some crystals, even when they are direct gap. Since the all samples studied were direct gap semiconductors which allowed the $k = 0$ transition to take place, details regarding absorption and emission processes for indirect crystals will not be covered in any detail.

2.3.3 Momentum Conservation

In addition to vertical transitions within the E-k diagram, a lateral shift may be involved if a change in electron momentum is provided by another process. These momentum-changing processes include electron-electron scattering, electron-impurity scattering, and phonon absorption or emission. Electrons which absorb or emit phonons, which are quanta of lattice vibrations, will undergo a small increase or decrease in energy for the respective processes along with a change in momentum. Details of phonon energies and distributions will be provided in the section on emission processes. Electrons scattering from other electrons may undergo an increase or decrease in momentum, depending on the momentum the other electron possesses and the incident angle for the interaction. It is to be noted that a semiconductor in equilibrium possessing phonons and free carriers cannot be at 0°K, assuming that it is non-degenerate. If a semiconductor is said to be degenerate, it has been doped heavily enough to provide for free carriers, even at 0°K. Impurity site scattering will lessen the energy of a carrier and provide some momentum change as well.

Electron-electron and electron-impurity scattering require a sufficient population of free carriers and of impurity sites, respectively, for each to proceed at an appreciable rate. Since a lateral shift is involved in the E-k diagram for these interactions, a variety of excitation processes is possible.

These types of excitation processes will proceed in at least two steps (photon absorption plus the scattering event), and will have a lower probability of occurring than any direct process that is permitted to take place. The probability of occurrence of these momentum-changing processes may be increased if the population of each of the intervening entities can be increased. Raising the temperature of a sample will increase the number of phonons present, and will also increase the number of free carriers. The number of free carriers will increase greatly if the sample is doped and the temperature is increased above 0°K. In this case, donor electrons can be thermally excited into the conduction band, and acceptor levels can be filled to provide for holes in the valence band with only minimal thermal energy. Crystal defects may also provide scattering centers, and can be introduced intentionally into the sample to allow for indirect transitions.

2.3.4 Absorption Within the Same Bands

Intraband absorption involves the excitation of carriers within the same band by a photon absorption process. A vertical transition may be possible since subbands can exist for many semiconductors. In III-V compounds, a number of subbands can exist within both the valence and conduction bands.

GaAs, in particular, possesses three valence bands which are identified as the light hole band, heavy hole band, and split-off band. When spin-orbit coupling is taken into account, these subbands may exhibit additional splittings. Transitions between subbands near the energy gap may then take place through a photon having the appropriate energy. Due to the small separation of the split bands, the photon wavelength would need to be somewhere in the infrared portion of the spectrum.

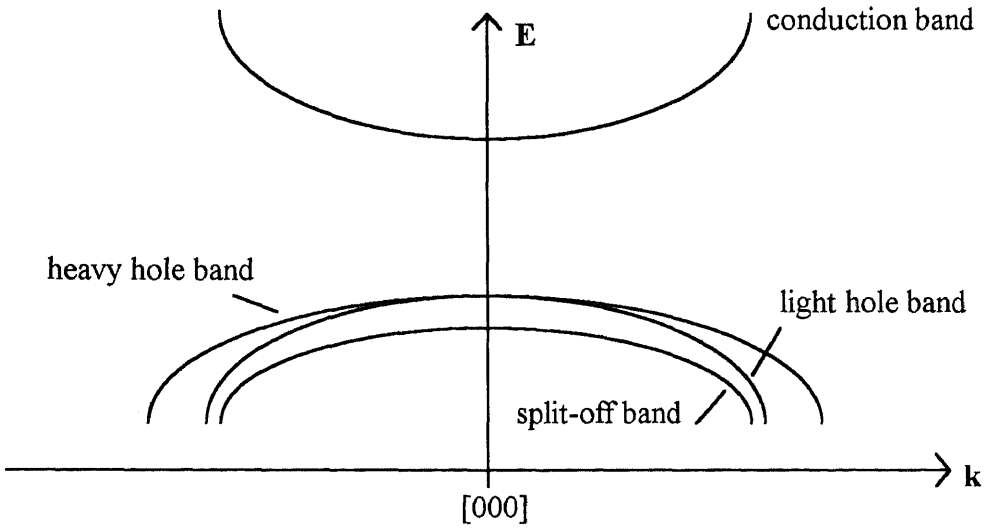

Figure 2.3 Subbands within the valence band for direct-gap semiconductors. The light and heavy hole bands are degererate at the center of the crystal, while the split-off band is separated by the energy due to spin-orbit interaction.

When a semiconductor heterostructure is created, the existence of subbands becomes important in analyzing carrier behavior. When a narrow gap semiconductor is sandwiched between layers of a wider gap semiconductor, carrier motion becomes quantized in the direction of carrier confinement.

Free carrier absorption also involves an excitation within the same band, but also within the same subband as well. It proceeds via a momentum as well as energy change, so it is either a phonon-assisted process or aided by electron scatteringfrom impurities in the sample. Free carrier absorption also takes place in the far infrared portion of the electromagnetic spectrum. Long wavelength photons excite the vibrational modes of the crystal lattice, providing thermal energy to the sample.

2.3.5 Exciton States

Lastly, exciton formation is another possible means of photon absorption within a semiconductor. Here, instead of the formation of an independent electron and hole within their respective bands, each may be bound to the other in a two-body entity. For free exciton

formation, the pair move together within the crystal tied together by a binding energy that is small in comparison to the energy gap of a given semiconductor. The small binding energies involved also mean that the pair may be easily dissociated due to thermal energy, and may not form if the sample temperature rises much above absolute zero. This binding energy lessens the energy that is necessary to create an electron-hole pair, so photons of an energy smaller than the bandgap can cause their formation. Thus the equation governing this process is given by

$$h\nu = E_g - E_x$$

with E_x being the exciton binding energy (on the order of meVs). In addition to free excitons, which exist in large numbers only in very pure samples at low temperatures, many bound exciton states are possible. When impurities are present in a crystal, the exciton is given the opportunity to lower its energy and may form another entity by binding with a donor or acceptor atom. It may also bind to another electron or hole to form a more complex system.

2.3.6 Impurities and Defects

The introduction of impurities into a sample will provide for discrete energy levels within the forbidden gap when the impurity concentration is low, and may form bands within the gap when the concentration of a given impurity state increases. Impurity bands may then merge with the valence or conduction bands and obscure their identity under some conditions. Different elements introduced into the sample will form separate energy levels for a given configuration within a crystal. An impurity atom may replace the semiconductor atom or it may lodge between lattice sites as an interstitial impurity.

Crystal defects will have the same effect as impurity sites in that new energy levels will form within the forbidden gap. Two possible defects are interstitials and vacancies. An interstitial defect is the same as an impurity interstitial, except that the atom off the

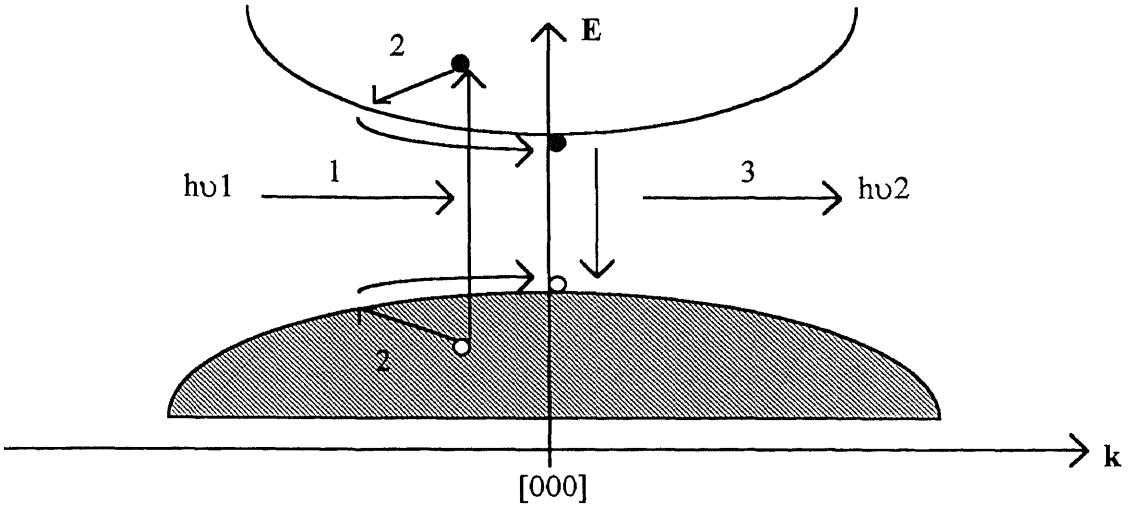

Figure 2.4 E-k diagram for luminscence process chain. 1) incoming photon of energy larger than bandgap creates electron-hole pair. 2) thermalization reduces separation energy of the pair, bringing them to band edges and near the k = 0 position. 3) recombination of pair to emit photon of smaller energy than excitation photon (near the band gap energy).

lattice sites is one which composes the crystal. These additional energy levels add to the complexity of absorption mechanisms that may be taking place via one of the aforementioned processes.

2.4 Typical Photoluminescence Chain of Events

Although many types of absorption and emission processes may take place within a sample being studied, only the most typical processes will be of interest since they will dominate. The samples are excited by a laser which provides for photons of an energy somewhat higher than the bandgap energy for the sample being tested. This will insure that all of the various recombination mechanisms will take place, since observation of these processes is the goal of the study. Due to this provision, the dominant mechanism will be interband absorption, where electrons are excited from the valence band edge well into the conduction band. The use of a light source having an energy larger than the bandgap means that it is possible to provide excitation for the many electrons that have k values different from zero

as well as those possessing a k value of zero. All crystals examined in this study permitted the k = 0 transition to take place, so the following absorption equation will apply to characterize the absorption coefficient (α):

$$\alpha(h\nu) = A^* (h\nu - E_g)^{1/2},$$

$$A^* \approx q^2 (2 m_h^* m_e^* / m_h^* + m_e^*)^{3/2} / nch^2 m_e^*$$

In this equation, E_g is the energy gap, q is the electronic charge, m_h^* and m_e^* are the effective masses for holes and electrons, respectively, and n is the index of refraction for the sample. This result due to work by Bardeen, Blatt, and Hall (1956). It is important to note that the absorption coefficient has a square root dependency for crystals allowing k = 0 transitions as the incoming photon energy is increased beyond the energy gap. This relation will show up again for free carrier emission spectra.

The allowance of a range of momentum values for the carriers undergoing excitation can lead to a large population of electrons in the conduction band and of holes in the valence band while the excitation source is turned on. For a sample at 0°K, the population of either carrier type will depend upon the excitation rate, the recombination rate, and number of available states for the electrons to move into. The rate of excitation is dependent upon the laser power, while the recombination rate is a summation of rates for all recombination processes taking place within the sample. If the excitation rate is sufficiently high, the instantaneous population of electrons in the conduction band may be equal to the number of available states for them to move into using a given photon energy. This means that increasing the output power of the laser beyond this point will not have any effect on the absorption or emission characteristics of the sample. Another way of stating this is that the crystal will be transparent to the laser at this point. If the excitation rate is not so high as to saturate the sample, then a typical excitation and emission process will involve the following.

An electron will be excited into the conduction band to form an electron-hole pair at the same point in k space. The energy separation of the pair will be equal to the energy the of the incoming photon. The electron and hole will then undergo phonon emission to shift their positions to the band edges since this is the most likely event to take place for carriers not at thermal equilibrium with the lattice. A sample at or near 0°K will have a negligible population of free carriers, and any which are created far from the band edges will emit phonons to lower their energy while continually changing their momentum vector. This free carrier scattering is also called thermalization, since the extra energy each carrier possesses above the gap energy is given up to the lattice as heat. Eventually the electron will reside at the bottom of the conduction band and the hole at the top of the valence band, where recombination may take place through a number of mechanisms. This three step process is illustrated in Figure 2.4. The mechanisms for these recombination events will be discussed in the next section, and follow the same rules introduced for absorption with regard to probabilities, rates, energy and momentum conservation.

2.5 Carrier Recombination

2.5.1 Introduction

The recombination of an electron-hole pair within a crystal will release an energy equal to the separation energy for the two entities. This process may occur radiatively, with the emission of a photon, or non-radiatively, by giving up the energy to the lattice. Radiative processes form the basis for photoluminescence studies, so only these transitions will be of interest.

As with absorption processes, many mechanisms exist to provide for a variety of possible photon emission energies. The dominant types of transitions to be expected will depend upon the relative rates with which all transitions proceed. Each rate will depend upon the probability that a given process will occur (P_{ul}), the number of filled upper en-

ergy states (n_u), and the number of empty lower energy states available (n_l). Using the notations as just defined, an individual rate can be written as

$$R = P_{ul} n_u n_l$$

with the value of P_{ul} determined by the type of transition and by the particular sample (Pankove 1971, 107). A summation of all of these rates gives a total recombination rate, with the dominant process proceeding at the highest rate.

A carrier's lifetime, τ, is the reciprocal of the total rate, so a small value of τ implies a high recombination rate. It is common to use lifetimes when speaking of carrier transitions, and a lifetime value may be assigned to each process as if it is the only one allowable. In this way, a comparison can be made between recombination mechanisms as far as which are to be expected to proceed at an appreciable rate. If one were considering only two processes, for example, a comparison can be made for the value of τ given to each one. If one lifetime is on the order of a few seconds while the other is on the order of microseconds, then the first process may be almost neglected since it will rarely take place.

2.5.2 Interband Recombination

The simplest mechanism for electron-hole pairs to recombine in a direct gap crystal is through a direct band to band transition. This process, the reverse of interband absorption, will produce a spectrum that is directly dependent upon the band structure of the sample being studied. It may also be referred to as free carrier recombination since a free electron and free hole are involved. The equation governing this process is

$$I(h\nu) = A^*(h\nu - E_g)^{1/2}$$

where $I(h\nu)$ is the light intensity and A^* is the same constant from the equation in Section 2.4 for direct gap crystal absorption (Bardeen, Blatt, and Hall 1956, 146).

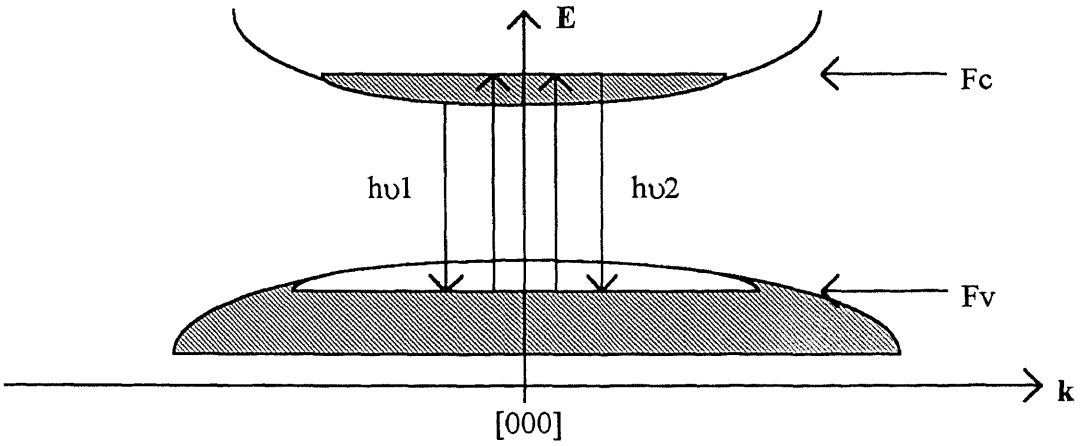

Figure 2.5 Band filling due to high excitation level. The semiconductor is at 0 K, but large incoming photon flux has populated the conduction band with electrons. The Fermi levels for conduction and valence bands have moved away from the center of the bandgap into their respective bands. Photons produced through carrier recombination can have any energy between hυ2 and hυ1.

A high enough level of excitation or high enough sample temperatures will cause band filling, and allow higher energy photons to be emitted (higher than E_g). Band filling by high level excitation occurs when the incoming photon flux is high enough to provide for an optical absorption rate which exceeds the total rate of recombination. Temperature dependence of carrier concentrations may be found for samples under excitation by using

$$n = n_i e^{(F_n - E_i)/kT}$$

$$p = n_i e^{(E_i - F_p)/kT}$$

in which n_i represents intrinsic carrier concentration, $F_{n,p}$ are the quasi Fermi level for electrons and holes, and E_i is the Fermi level for an intrinsic sample (Streetman 1990, 110). The degree of excitation will determine the deviation of F_n and F_p from E_f. Both high level excitation and temperature increases will each give an exponential increase in the number free carriers to fill the band states, thus providing for a spectrum peak that is widened and shifted. The low end of the interband spectrum is at E_g, since an electron-hole pair cannot move closer together than the bandgap separation (when considering only this direct mechanism for recombination). Band filling as described here, while desirable

for semiconductor laser operation, is not desirable for photoluminescence studies since it will obscure near-band edge transitions. An illustration depicting band filling is given as Figure 2.5.

The bandgap will have a temperature dependence as well, arising from the changes in lattice constants with thermal energies possessed by the crystal atoms. For many semiconductors, the bandgap will decrease with increasing temperatures, and may be written as the function

$$E_g(T) = E_g(0) - \alpha T^2/(T + \beta)$$

with $E_g(0)$ being the bandgap at 0°K and α and β being constants. For GaAs, the constants are $\alpha = 5.405 \times 10^{-4}$ eV/K^2 and $\beta =$ 204 K, with $E_g(0) =$ 1.519 eV. Both formula and constants are from Blakemore's publication (1982).

The formation of impurity states within the band due to doping and/or defects will widen and shift the spectrum peak, since more transitions will be permitted to take place involving lower energy photons. Due to the high efficiency of luminescence arising from such impurities, free carrier recombination becomes difficult to discern (Gilleo, Bailey, and Hill 1968, 899). Also, excitation levels which are too intense will produce enough free carriers that may cause electrical shielding, and screen out free carrier recombination lines in a spectrum (Wright 1966, (unpublished), Casella 1963, 1703, and Mahan 1967, 882). Only with minimal excitation levels, sample temperatures very near 0°K , and extremely pure crystals can a sharply peaked band to band recombination emission be seen about the bandgap energy level.

2.5.3 Impurity Levels

The introduction of impurities, also called dopants, into a semiconductor is usually essential to shape its electrical and optical properties. In addition to these intentionally added impurities, unintentional impurities are usually present in III-V compound crystals and alloys due to uncontrollable reactions during processing. As stated previously, one of

Table 2.1 Binding Energies for Acceptors Identified in GaAs Samples.

impurity	binding energy (meV)	information source
carbon	26.0	Ashen, *et al.* (1975)
silicon	34.5	"
germanium	40.4	"
zinc	30.7	"
cadmium	34.7	"
beryllium	28.0	"
magnesium	28.4	"
tin	171	Schairer and Grobe (1970)
lithium	23	Milnes (1973)
gold	90	"
manganese	95	"
silver	110	"
lead	120	"
cobalt	160	"
nickel	210	"
copper	23	"
iron	37	"
chromium	630	"

the principal uses of photoluminescence studies is to characterize sample impurities. Samples which have not been intentionally doped can be examined to determine which substances have been incorporated into the growth process. This information may then be used to track how the impurities may have entered and how they may be reduced if they produce unwanted transitions.

For a III-V compound such as GaAs, each impurity can give rise to a given energy level within the bandgap to establish it as a donor or acceptor, depending on which element it is replacing in the lattice. For example, a silicon atom (from column IV in the periodic table) replacing a gallium site in the lattice (from column III) will provide for a weakly bound extra electron and therefore form a donor state. A carbon atom (from column IV) replacing an arsenic site in the lattice (from column V) will leave a hole at a specific energy level within the forbidden gap. The resulting electron or hole will be weakly bound to the site and may be released as a free carrier using small thermal energies when

the donor or acceptor level is shallow (close to the band edges). This binding energy can be approximated as

$$E_i = m^* q^4 / 2h^2 \varepsilon^2 n^2 = (m^*/m\varepsilon^2 n^2) 13.6\ eV$$

using a hydrogenic atom model (Pankove 1971, 9). A donor impurity in this model is equivalent to a hydrogen atom immersed in a medium having a dielectric constant ε, which is the constant for the semiconductor being considered. A similar consideration may be made for holes using the appropriate value for their effective mass, m*.

The ratio of effective to rest mass, m^*/m, becomes an important quantity since this varies considerably for different semiconductors and for electrons and holes within the same material. In GaAs, the hole to electron effective mass ratio is about eight to one when considering heavy holes. This implies that the acceptor levels are typically about eight times the distance from the band edge than the donor levels, and would be much easier to discern. In GaSb, this ratio is higher, so donor levels are even closer to the conduction band edge. It is for this reason that most photoluminescence work for these semiconductors concerns acceptor identification. A number of acceptors which have been identified in GaAs samples are listed in Table 2.1. Donor levels are so shallow that it becomes very difficult to identify individual levels, or to even recognize them separately from transitions taking place at the conduction band level. The presence of both donors and acceptors within a sample will complicate the allowed emission transitions that will be taking place during photoluminescence.

2.5.3.1 Impurity Level Transitions In addition to the excitonic complexes that may form due to impurities, there can be five other transitions taking place, when considering free carriers. These are illustrated in figure 2.5. Two of these transitions are from band edge to the respective impurity level. These include an electron from the conduction band moving into an empty donor level (provided by an ionized donor) and a bound electron in an acceptor level (provided by an ionized acceptor) moving into the valence band. These

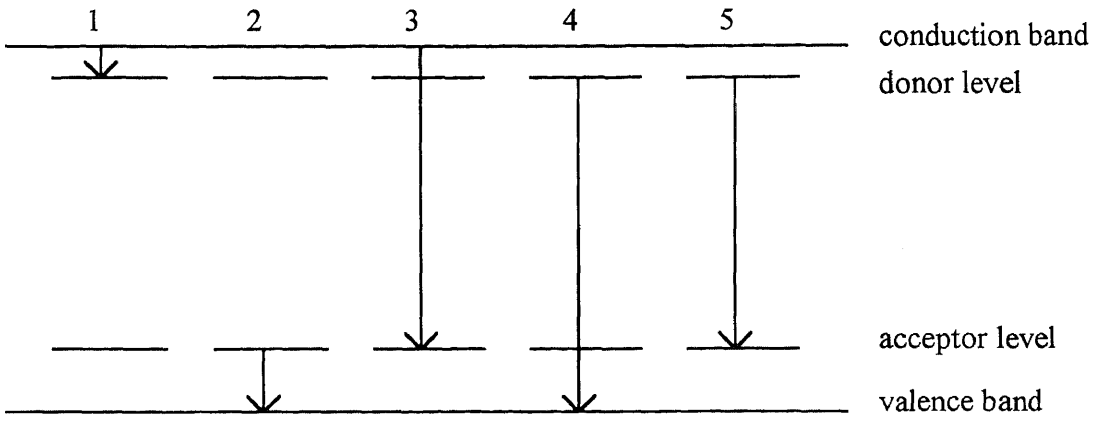

Figure 2.6 Impurity level transitions within a semiconductor possessing both donor and acceptor levels. Processes 1 and 2 are shallow level transitions. Processes 3 and 4 are both free to bound (FB) transitions, with number 3 being more readily seen when donor levels are shallow. Process 5 is a donor-acceptor (DA) transition.

low energy transitions have been suggested to take place through mostly phonon emission, and therefore are not radiative (Pankove 1971, 132). In any case, the low energies involved make studies very difficult so that they are not of any interest here. Two other transitions that may be seen are from far band edge to impurity level. An example is an electron moving from conduction band to hole at an acceptor level. This is frequently called a band to acceptor (BA), or free to bound (FB) transition since a free electron moves into the impurity bound state near the valence band. The other transition, involving an electron moving from a donor level to the valence band, is much more difficult to see (due to the shallow donor levels) and is not discussed in research work to any great extent. This transition would only be detected when using temperatures near that of liquid helium and having available high enough resolution to distinguish this process. Lastly, there may be transitions between donor acceptor levels (DA transitions), which provide photons of an energy less than the band gap due to a reduction from the binding energies of both donor and acceptor levels. Details of this process are given in the next section.

2.5.3.2 Free to Bound versus Donor Acceptor Recombination FB and DA transitions are related in some materials, and their identification may be made by varying sample temperature to obtain several spectra for comparison. Through the work of Leite and DiGiovanni (1966), Ashen, *et al.* (1975), and Swaminathan, *et al.* (1985) using GaAs samples, the emission process can be seen to shift from DA to FB as sample temperature is increased. This is a result of the ionization of the shallow donors (about 3 meV below band) into the conduction band in the temperature range of approximately 2 to 20°K.

At temperatures near that of liquid helium (4.2°K), most of the donor electrons would be frozen into their donor states and allow for the DA transition to be seen. As the sample temperature increases, the electrons are excited into filling the nearly empty conduction band so that many more FB transitions would take place. The DA emission will provide photons of an energy given by

$$h\nu = E_g - (E_a + E_d) + q^2/\varepsilon r$$

with $E_{a,d}$ being the acceptor and donor energies and r being the separation distance for the two impurities involved (Thomas, Gershenzon, Trumbore 1964, A269). The equation shows that the photon emission energy is lessened by the binding energies of the electron and hole due to the impurity sites and increased by a Coulomb interaction energy, given by the last term.

The identification of a DA transition may be made due to the widened peak from the last equation term. A variation of the distance r from donor to acceptor throughout the sample will widen the DA emission energy accordingly, and this energy spread may lead to an easily recognizable peak shape. If, however, the dielectric constant term, ε, is small, then the widening will be diminished and the peak shape may not be as distinguishable. For very large values of ε, individual transitions may appear within a spectrum due to the fixed values for r. The intersital distance r will vary by fixed distances for a crystal, and equipment resolution may not be good enough to show the individual transitions unless the dielectric term becomes large enough.

An FB peak should appear narrow by comparison, but not as narrow as a well-defined peak due to a bound exciton state. The FB transitions due to one type of impurity will not have a single definitive transitional energy since the free carrier energy level may vary. While the acceptor level for one impurity may be well-defined for a given sample, the free carrier energy can take on a continuum of values above the band gap energy, dependent upon sample temperature. A low donor level and low excitation level for the laser used in photoluminescence studies will reduce this peak widening somewhat. The identification of a particular impurity may be made using a well-defined FB peak by using

$$E_{FB} = E_g - E_a$$

in which the E_a term represents the acceptor level. Comparison of a calculated value for E_a within an experimental spectrum to known acceptor energy levels will produce several possible candidates for the impurity which is likely to have caused the FB transition seen.

2.5.4 Phonon Behavior in III-V Semiconductors

Before discussing phonon assisted emission processes, phonon behavior within III-V compounds will be outlined. All material in this section is from Kittel (1986). Phonons, which are quanta of lattice vibrations, will act as if they possess physical momentum of magnitude $hk/2\pi$. Solutions for the equation of motion of a lattice of atoms undergoing vibrations yield a plot of allowed frequencies versus wavevector (ω versus k). This plot is similar to the E-k plot for free carriers since $E = h\omega/2\pi$ for phonons.

When a semiconductor consists of two atoms per cell unit, as does GaAs, two distinct branches of the ω versus k diagram appear. The two curves which form have been given the names optical and acoustical branches, and will have distinctly different dependencies on wavevector. The acoustical branch approaches zero linearly as k approaches zero. However, the optical branch will not approach zero. Instead, it increases slightly in ω as k approaches zero, and therefore its energy will be greatest at this point. This fact is

of importance here since transitions about $k = 0$ are considered for all processes in this study of III-V compounds. Therefore optical phonons may take part in transitions to be discussed, while acoustic phonons will not.

In addition to this distinction, three modes will exist for each branch corresponding to the direction of travel of the propagating wave in relation to the crystal planes. For a given crystallographic direction, one longitudinal and two transverse modes will then exist, each possessing different energies.

2.5.5 Phonon and Carrier Assisted Processes

The process of photon emission may involve a momentum change for the electron undergoing the transition in certain cases. Phonon emission or absorption and carrier interaction are two possible processes which may provide this. While phonon emission or absorption must take place in an indirect transition, this process has a lower probability of occurring than a direct transition.

A comparison in probabilities for various recombination events can be made from the time constants assigned to each. Within a band, optical phonon emission occurs on the order of 1×10^{-12} s (Tatham, Ryan, and Foxon 1989, 1637, Grahn, *et al.* 1990, 2426, Jain and Das Sarma 1989, 2305, and Ridley 1989, 5282), acoustic phonon emission takes place within about 3×10^{-10} s (Kastalsky, Goldman, and Abeles 1991, 2636), and band to band radiative recombination proceeds with a time constant of about 1×10^{-7} s (Yariv 1975). These values only apply to free carriers, since a carrier at the band gap edge is not likely to emit phonons. The reason for this lies in the low energy value each phonon possesses, which would not carry a carrier across the energy gap unless a cascade of phonons is emitted to achieve this (an unlikely event).

Due to the small time constants for thermalization versus those for emission, most electron-hole pairs will be at the same point in momentum space, at the band gap energy level. Such a configuration will only allow for vertical transitions that photon emission

will provide. In order to observe phonon intervention in photoluminescence, a phonon emission must take place while a radiative transition is taking place. While there is a likelihood of this taking place, the small rate of the occurrence as compared to other processes make this identification difficult. One study conducted by Leite and DiGiovanni (1966) has shown that, under carefully controlled conditions, phonon assisted processes may be identified. They show up as replicas of some original recombination lines within a spectrum, shifted down in energy by the amount the phonon possessed. Their results showed a shift of 36 meV per longitudinal optical (LO) phonon emitted for one and two phonon assisted processes which they could identify, replicating a bound exciton emission.

Carrier scattering may also provide a momentum and energy shift for the recombining electron or hole. In direct gap materials, this indirect process will again have a low probability of occurrence, and may not be seen due to other competing processes. It may be possible for an electron to undergo the reverse process described in Section 2.3.3, in which an electron at the bottom of the conduction band scatters from another electron, giving it a momentum and energy boost to send it higher up into the conduction band. The first electron will then exist in a virtual state within the forbidden gap after losing energy and momentum. It is possible to exist at this forbidden energy for a short time due to the uncertainty relation in quantum mechanics which can be written as

$$\Delta E \Delta t \geq h/2\pi$$

If the time an electron exists at a forbidden level is very short, the uncertainty in its energy can be large, and will allow it to exist within the band gap. From this forbidden energy level, it may then decay by recombination with a hole in the valence band. A direct gap crystal may require a phonon to shift the momentum of the electron back into a zero k value, so it will be a three step process. This will reduce the likelihood of seeing carrier assisted processes for direct gap materials to a level less than that for simple phonon

assisted recombination. Although both of these processes have a low probability of taking place, it may be possible to see them with certain pure crystals as a lower energy transitions within the bandgap of the sample that direct transitions would not account for.

One last consideration which needs to be made in this regard involves non-radiative processes due to carrier interaction. When the population of free carriers becomes relatively large, Auger recombination may take place (Peierls 1932, 905). In this case, the energy of a recombining electron and hole which normally manifests itself in the form of a photon is instead given to another electron. The free electron which receives the energy will be excited well into the conduction band and give up energy in the form of phonons. It is also possible to have a variety of excitation possibilities, such as excitation of an electron from deep within the valence band to the valence band edge, or from a donor level into the conduction band, or from deep within the valence band into an acceptor state. The important point is that no photon emission results from these transitions, and they are more likely to take place when the free carrier density is high. Therefore, samples studied at higher temperatures are expected to have a luminescence intensity which is low compared to the same samples taken at low temperatures. Since most photoluminescence studies are concerned with crystal structure of the sample itself, carrier interaction is not desirable, so it is reduced by employing low temperatures and keeping the excitation source at a minimum.

2.5.6 Exciton Recombination

The possibility of the formation of electron-hole pairs with an energy less than the band gap energy was introduced in Section 2.2.6. Electron-hole pairs may also form excitons by lowering their energies from some excited state which is larger than the bandgap energy. Instead of the band gap edges being the lowest attainable energy state for the electron and hole to decay into, they may lower their energies further still by forming an

exciton. If the pair recombine, the light emitted is lower than the bandgap energy by the binding energy of the exciton, which is given by

$$E_x = -m_r^* q^4/2h^2\varepsilon^2 n^2$$

where n is the quantum energy state for the system (n=1, 2, 3, ...) and m_r^* is the reduced mass for the electron and hole. This value is used since the two bodies orbit about their common center of mass, and it is given by

$$1/m_r^* = 1/m_e^* + 1/m_h^*.$$

The value of the n = 1 exciton binding energy for GaAs has been estimated to be 4.4 meV (Sturge 1962, 768) and 5.25 meV (Wright 1966, (unpublished)) for two different sources.

For excitons to exist, a sample must be at a low enough temperature so that thermal energy does not overcome the small exciton binding energy. Free exciton transitions will not be easily seen in many samples, since impurities and crystal defects will permit an electron-hole pair to lower its energy again by binding to another entity.

Specific emission lines will depend upon what the pairs have bound themselves to and upon which excited state they existed in when they recombined. There may also be a multiplicity of exciton emission lines due to phonon emission accompanying exciton recombination. Exciton emission lines are characterized by narrow linewidths in an emission spectrum in comparison to other emission processes. This is a result of the specific energy state in which they exist prior to recombining. In GaAs, bound exciton lines are usually found to be much narrower than free exciton recombination lines. In one study of GaAs at a temperature of 1.4°K, typical widths of bound versus free exciton lines were found to be .1 meV and 1 meV for each process, respectively (Gilleo, Bailey, and Hill 1968, 898). It is the intensity and width of these emission lines which provide a valuable clue as to the crystal quality and impurity distribution in the sample being studied. A general form for a bound exciton recombination process can be written as

$$h\nu = E_g - E_x - E_b - nE_{p,m}.$$

A photon's energy is lowered from the band gap value by the energy of the free exciton (E_X), the exciton binding energy (E_b), and by n phonons emitted during the process which are of mode m ($E_{p,m}$). A more complex expression may be written if phonon absorption is permitted to take place when multiple numbers of mixed phonon modes are involved.

2.5.6.1 Free Exciton Recombination In order to observe the recombination due to free excitons, the same considerations apply to a sample with regard to purity, low temperature, and low excitation levels which were discussed for free carrier recombination. If it becomes possible to observe free exciton lines within a spectra, then these lines may be used as reference points in a III-V semiconductor scan since they will be independent of any impurities that may be present (Gilleo, Bailey, and Hill 1968, 900). Another observation to be made is that while the n=1 exciton line may be difficult to observe, any higher order lines will decrease in intensity as $1/n^3$, so that they will be still more elusive to find within a spectra (Elliot 1957, 1384). Typically, only at liquid helium temperatures and below can the population of free excitons be sufficient to allow for their observation through recombination radiation (Gilleo, Bailey, and Hill 1968, 899).

2.5.6.2 Bound Exciton Recombination Many semiconductor samples will contain sufficient impurities as to mask any free carrier or free exciton lines, so that the dominant exciton recombination mechanism is through bound exciton (BE) emission. Their binding energy is a sum of the free exciton energy and the energy binding the exciton to the impurity or defect. Sample quality is reflected in the intensity of bound exciton peaks and their widths.

Different impurities will act as killer centers for bound exciton emission since they readily capture free carriers, and fluctuations in sample composition or the existence of crystal defects will act to broaden the transition energy for a particular bound exciton

emission. A large number of crystal defects will deform the periodic potential of the sample, and may even cause dissociation of most exciton pairs before they can recombine.

In principal, under high spectral resolution, the sharpness of the exciton peaks could be an aid in attempting to pinpoint the type of impurity it is associated with. By impurity type, this refers not to the particular element or compound but whether it is a donor or acceptor and whether it is neutral or ionized when bound excitons recombine due to its presence. A study of bound exciton emissions was performed by Ashen, *et al.* (1975) using a number of GaAs samples which were intentionally doped. It was found that, with the exception of tin, being a deep level acceptor, all of the other impurities produced bound excitons of an energy $1.512 \pm .001$ meV. This represents a binding energy of about 7 meV for any bound exciton state, independent of the impurity. The small deviation among them was likely due to experimental factors, so that most all impurities will not be able to be identified by the position of the bound exciton peak. Free to bound transitions are a better indication of the impurity involved, while exciton peaks may be used merely to characterize the overall crystal quality and extent of impurity energy levels the sample contains.

CHAPTER 3

EXPERIMENTAL SETUP

3.1 Introduction

A detailed figure of all apparatus used to gather data on the samples is given on the following page (Figure 3.1). The equipment necessary for photoluminescence study may be broken down into four groups for discussion. They will include the excitation source, sample containment, optics, and signal readout with data acquisition. As a whole, the setup provided for photoluminescent spectra data to be taken in real-time as a function of sample temperatures, and to provide for a hard copies of data in the form of plots to analyzed at a later time. The incident light beam from the laser, reflected laser light from the sample's surface, and the photoluminescence signal ray to be analyzed are given by thin-line arrows in the diagram.

The incident beam proceeds from the laser source to be reflected by two mirrors, passes through a filter, is chopped by a rotating blade, and focused by lens 1 onto the sample. The reflected beam plus photoluminescence produced near the sample surface passes through the cryostat window, and was focused by lens 2 onto the monochromator slit. Inside the monochromator, the radiation is dispersed and a selected frequency emerges from the exit slit and to be picked up by the light detector. Signal connections between equipment are indicated as well for clarity.

3.2 Excitation Source

The source for sample excitation was an Omnichrome 532 Series argon ion laser which provided a dominant transition wavelength of 514.0 nm. A total of nine transitions were possible, and they were given as 454.0, 457.0, 465.0, 472.0, 476.0, 488.0, 496.0, 502.0,

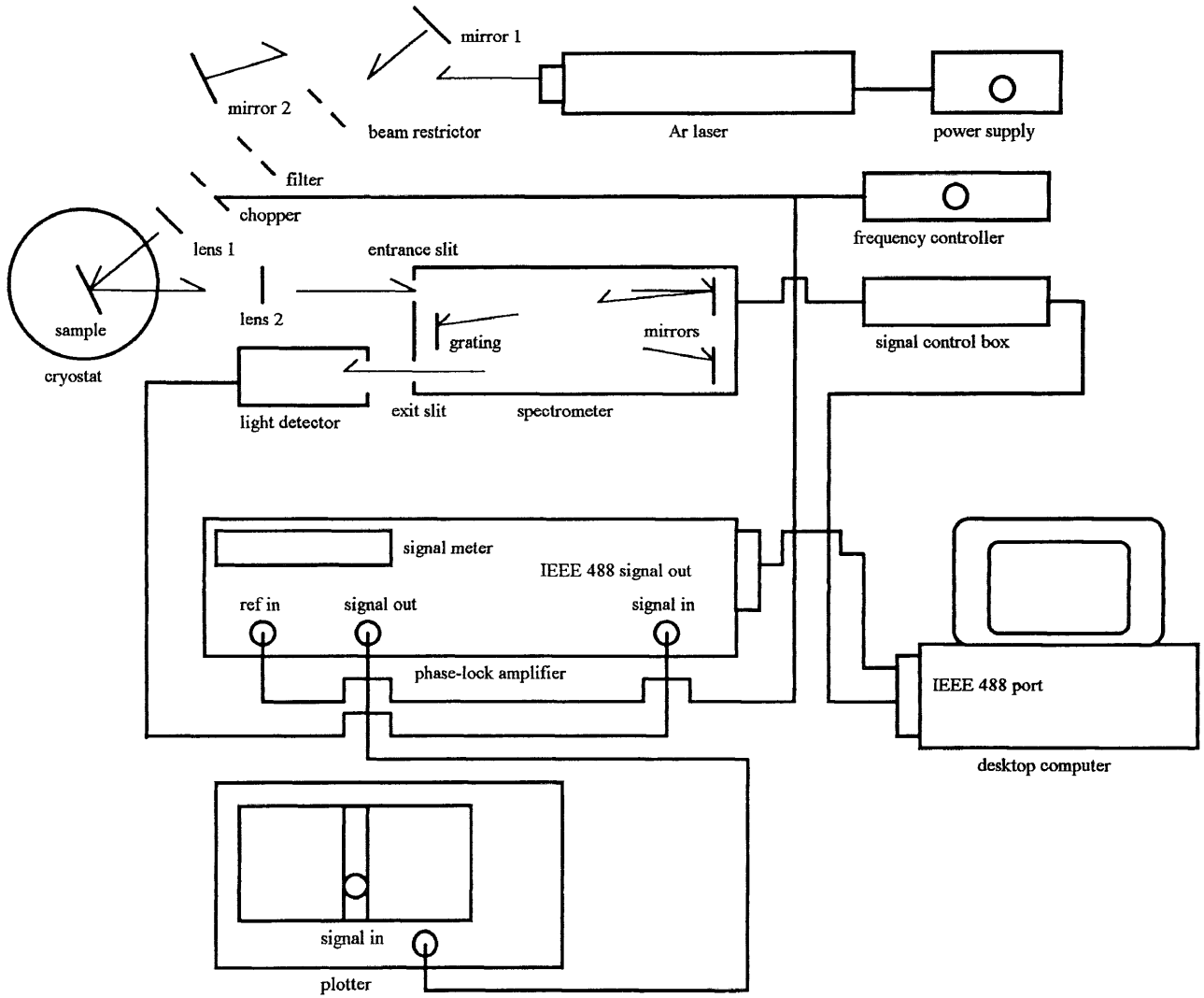

Figure 3.1 Experimental setup for low temperature photoluminescence study.

and 514.0 nm. The strength of each of these lines is a function of power supplied to the laser and the laser head configuration, which was set to enhance the single line at 514.0 nm. To minimize multiple transitions, relatively low laser power was utilized as well.

Despite these precautions, other emission lines were observed due to many non-lasing transitions that can occur in the gas discharge. The basis for this speculation lies in an analysis of a spectrum taken using an aluminum target without a filter in place along the light path. Since this sample provided only for reflected light, the complex spectrum obtained must have emanated from the laser source and could not be accounted for by laser transitions alone. Placement of a filter in the path of the incident beam was necessary to eliminate these extraneous lines.

3.3 Sample Containment

In order to provide the low temperatures necessary for the samples being studied, a cryostat was employed. This consisted of an airtight chamber with windows to allow for light transmission in the wavelengths of interest, a sample mount in the center of the chamber that served as a heat sink, and a compressor for lowering the temperature of the sample mount. A Leybold-Heraeus compressor provided a four stage compression/ expansion cycle using helium gas to cool the sample mount, called a cold head, down to a lower limit of 10°K.

While other means of sample cooling exist, some advantages exist with this setup. Other methods of cooling include immersion of the sample in liquid nitrogen or helium, which causes considerable bubbling around the sample holder. The bubbling may interfere with the excitation beam and photoluminescence light, causing distorted signal readouts. In addition, temperature control can be more difficult using these arrangements, as the temperatures of the liquids are constant at 77.4°K and 4.2°K for nitrogen and helium,

respectively. Liquid helium is particularly difficult to work with due to its high cost and tendency to boil vigorously, which must be controlled to avoid interference with the incident light beam or the photoluminscence light.

To provide for insulation for the setup used here, the chamber was pumped down to a range of about 10^{-3} Torr by a mechanical pump which was turned off prior to cooling the sample. A container of activated carbon granules served to absorb remaining gases which helped to eliminate condensation on the chamber windows caused by heat conduction through these gases inside the chamber.

After reaching the lower temperature limit, a resistive heater was used to raise the sample temperature. A set of wires carrying low current were twisted around the cold head and fed a controlled signal to set the sample temperature desired. In order to monitor the cold head temperature, a silicon diode temperature probe was also in contact with the sample holder to feed a signal back to the heater control unit.

3.4 Optics

3.4.1 Discrete Components

A series of lenses, mirrors, a beam restrictor, and a filter were needed to modify the incident light, reflected light, and photoluminescence signal. The two mirrors used merely shortened the length of table needed to set up the equipment and provided height adjustment of the beam entering the cryostat by reflecting the laser at adjusted angles. After being reflected from the second mirror, the beam passed through an adjustable restriction device which controlled spot size. Following this, the beam passed through a bandpass light filter to eliminate intensity of all lines but the one dominant laser transition line at 514.0 nm. The bandwidth specification for the yellow-green filter was given as 514.0 ± 10.0 nm so that this single laser transition could be isolated. If long wavelength lines in the vicinity of the spectrum had been permitted to pass and be scattered from the sample, this would have produced complex, confusing results that may have been easily misin-

terpreted. A convex lens provided for focusing the incident beam onto the sample in a tight spot to insure that the sample frame or other cryostat fixtures were not illuminated by the laser. This would eliminate any stray signals coming from anything other than the sample itself. Lastly, a second convex lens was needed to focus the reflected and photoluminescence light onto the monochromator slit. The internal optics of the monochromator will be discussed in the next section.

3.4.2 Monochromator

A monochromator is used to provide a single wavelength of light from a source which contains many wavelengths, or may contain a continuum. In this study, an HR-320 monochromater manufactured by Instruments SA, Inc. was employed.

The heart of the instrument is the diffraction grating, which performs the wavelength selection. A diffraction grating is merely a glass plate which has many closely spaced parallel lines engraved in its surface, and may be coated with other materials to enhance optical efficiency. The spaces between lines allow light to pass through, so the grating acts as many-slit light source. Incident light will be focused by a concave mirror onto the grating, and light passing through the grating will be reflected by its back surface to be focused by a second mirror onto the exit slit. A beam of light incident upon a grating with d lines per cm, when focused at an angle of θ degrees with respect to the grating's surface normal, will show an intensity pattern that is a function of the beam's wavelength after emerging from the grating. Although the process governing the monochromator's selection is more complex than a transmitting grating since a beam enters, reflects from the back of the grating, and then exits, the basic concept is the same as a pass-through selection. A transmitting grating will be first discussed since the mathematics are too involved for the reflection grating to make clear the wavelength selection process involved.

The equation giving the maxima for a normal beam of light passing through a transmitting grating can be written as

$$d \sin \theta = n \lambda \quad (n = 0, 1, 2, 3, ...)$$

with n being the order of the grating used, d being the grating slit density, and θ being the angle, with respect to the grating's surface normal, at which the transmitted light is focused onto a spot for examination of light intensity. To use a pass-through grating for selection, the point at which one views the exiting beam must be altered while the incident beam is always normal to the grating. In contrast, rotation of a reflecting grating with respect to the incoming beam will cause the wavelength selection to be made.

The consequence of having an order number means that integral multiples of a given wavelength are also selected. This is not a problem in photoluminescence studies, since most processes of interest take place within a wavelength band which is narrow compared to the spacing of multiple orders. In order to determine the resolution that the grating can provide, a set of two equations are combined to make this estimation. The manufacturer quotes the resolving power as

$$R = \lambda/\Delta\lambda = nN/2$$

where λ is the wavelength being selected, $\Delta\lambda$ is the spectral resolution, n is the order used, and N is the number of lines on the total area of the grating. For GaAs and AlGaAs samples, the luminescence light was expected to be in the region of 6000 to 8000 angstroms, so a grating was used which had 1200 lines per mm. For the GaSb sample, a grating was needed which had a larger grating constant since the bandgap energy was farther in the IR region (about 1.5 μm). The grating used in this case had a density of 300 lines per mm. The spectral resolution was found by solving for $\Delta\lambda$ for each grating as follows:

$$\Delta\lambda = \lambda/R = 2\lambda/nN.$$

The total number of lines, N, was found by multiplying the line density by each grating's width of 68 mm. For the 1200 lines/mm grating, this equation gave a value of .17 angstroms. For the second grating of 300 lines/mm, the resolution was found to be 1.47

angstroms. These values represent the absolute limit for resolution, as other factors will enlarge these values considerably, notably the necessity to open the slits to obtain sufficient intensity.

To control the selected wavelength, an on-board stepping motor was used in conjunction with a desktop computer and control box. The computer provided a software interface for user supplied values of wavelength selections and scan speeds for the monochromator. This data was used to send the appropriate signals to the control box via an IEEE 488 port. The control box then provided a pulsed waveform to the mono-chromater's stepping motor input. The frequency of the pulsed waveform directly controlled the speed of the scan.

To achieve this type of control, two types of spectral calibration needed to exist. The first type concerns the agreement between the mono-chromater's readout scale and the actual position of the grating inside. A mechanical roll-over scale gave the wavelength selected for the current grating position, assuming that a 1200 line/mm grating was being used. The second calibration involved giving the software the grating's position every time the program was started. The monochromator had no way of conveying the current grating angle, since its position was controlled in a relative manner by pulse frequency from the control box. Although the second calibration insured that the software read the exact value of that on the meter, the first calibration could only be done at the factory or by a qualified technician. Therefore internal misalignment could have been a possible source of error here.

3.5 Signal Readout and Data Acquisition

In order to obtain a relative intensity of photoluminescence signals from each sample, an appropriate light detector was used in conjunction with a lock-in amplifier to maximize signal-to-noise ratio. For a permanent record of data, a plotter was connected to the lock-

in amplifier to provide a pen plot of signal strength. In addition, the signal from the amplifier was also fed directly to a desktop computer so that data could be stored digitally. The computer's main purpose was to control the monochromator wavelength selection, so data acquisition was a secondary task for it. A problem with software configuration prevented any digital capture of signal strength, so all data was taken by analog plots. The most important components for the job of signal readout were the detector and the phase-lock amplifier, so they will each be discussed separately in some detail.

3.5.1 Light Detector

In order to capture the light provided by photoluminescence processes within a sample, an appropriate light detector must be chosen. There were two types chosen for the two ranges of photon energies to be scanned. For GaAs and AlGaAs, a photomultiplier tube was used, and for GaSb, a semiconductor detector was employed.

Photomultiplier tubes operate on the basis of the photoelectric effect, in which an electron can be emitted from the surface of a conductor due to energy transfer from an incoming photon. A photosensitive cathode provides a source of electrons from an incoming photon flux by this method. The emitted electrons are then accelerated toward a series of charged plates called dynodes. Each dynode may emit several electrons for one incoming electron, so signal amplification is provided in this way. The last dynode provides the signal out in the form of a current pulse, with one pulse provided due to each incident photon. Photomultiplier tubes can be chosen for a particular wavelength range, since their sensitivity depends upon the type of material the photosensitive cathode is constructed of.

For longer wavelength studies needed for the GaSb sample, a PbS crystal detector was used. The bandgap of undoped PbS is about .37 eV at 300°K, or 3.35 μm in wavelength. The detector using this material was said to have a responsivity which peaked at about 2 μm, so this was an appropriate choice. An important distinction to be made

between the two detectors used was that the response time for the PbS crystal was considerably longer than that of the photomultiplier tube. This would have an effect on the resolution that can be seen for a given scan speed, and adjustment to the time constant for the lock-in amplifier needed to made when switching between detectors. Semiconductor detectors may be broken down into three types, which are photovoltaic, diode photoresister, and straight photoresister. The PbS detector was a straight photoresister type. Basically, the principal behind operation was that photoinduced electrons and holes will provide a current dependent upon incident light intensity.

3.5.2 Lock-In Amplifier

When a relatively weak signal needs to be obtained from a high noise level input, lock-in amplification is a commonly used tactic. The basic concept is to give the signal of interest a well-controlled frequency by which it can be found through a tuning circuit, then amplified. To achieve the frequency needed for the photoluminescence signal, the incoming laser beam was chopped by a rotating blade which was controlled by a frequency control unit. A control line from the unit was routed to the chopper while a frequency reference signal of the same chopping frequency was sent to the lock-in amplifier. This provided the amplifier the reference it needed to search for photoluminscence light among the light noise from other sources about the room. The detector fed the raw analog signal into the lock-in, which then sifted out a signal matching the frequency of the reference signal. The resulting signal was given as a reading on an analog meter and converted to a digital reading for display on an LED.

The necessary user-supplied control over the reading the amplifier provided included fine tuning frequency adjustment, signal readout scale, and signal time constant. Fine tuning was necessary to maximize the signal the amplifier read, as small delays from the sample luminescence due to laser excitation would exist. The tuning was angular in scale, so tuning 90° out of phase should produce a reading of zero. Fine tuning was em-

ployed to achieve this when necessary, and the coarse tuning was then set back to its original value. The scale reading was adjusted to obtain as close to a full scale reading as possible for the maximum signal size that was expected, without overloading the meter. Readings that were close to full scale would provide for more accurate output, and easier analysis of the resulting plot. Lastly, time constant adjustments were necessary in order to minimize signal fluctuation. These fluctuations take place due to variations in the rate of recombination mechanisms within the sample and, more directly, due to variations in the readout provided by the detector. If the signal provided by the detector is varying rapidly, a time constant must be chosen which is long enough to average out large, rapid fluctuations so that a relatively smooth signal is provided. This must be done carefully, as choosing a time constant too large will mask any sharp transitions which the detector may be capable of picking up.

CHAPTER 4

EXPERIMENTAL RESULTS AND DISCUSSIONS

4.1 Goal of the Study

The goal of obtaining spectra for analysis of the III-V semiconductor compound films used in this study was to characterize the quality of the MOCVD produced layers. A number of GaAs and AlGaAs films along with a GaSb sample were provided by a manufacturing laboratory for the purpose of providing an insight into the material quality. The GaSb sample is of particular interest, since GaAs along with AlGaAs have been studied extensively over the past several decades, while GaSb has not been researched to the same extent. Each of the samples used in the spectral analysis consisted of MOCVD films formed upon a bulk substrate formed by another process such as by LPE. The GaAs and AlGaAs samples were grown on GaAs and the GaSb sample was grown on bulk GaSb.

The interest in producing quality GaAs and AlGaAs films is partly due to their potential application in optical devices requiring direct gap materials, such as in semiconductor lasers. The use of these films for electrical devices is also of interest, due to the high speed in which they may operate owing to the low value of effective mass for electrons in GaAs. The same attributes apply to GaSb, with the important distinction that the bandgap is smaller for this semiconductor. Use of GaSb or a ternary semiconductor such as AlGaSb may be possible for a detector or laser operating farther into the IR region than a GaAs-based device (up to about 1.8μm at room temperature). The purpose of high quality thin layer production for the films studied here was to incorporate them in heterostructure laser devices. The first step in achieving multiple layer designs which operate with high recombination efficiencies is to have good quality layers which comprise the design. This study provided such an insight into the individual layers intended for this use.

4.2 Experimental Procedure

A number of samples produced by the same laboratory using their MOCVD process were scanned using the equipment depicted in Figure 3.1, and of these, four spectra were chosen for discussion. A scan for a particular sample at low temperature involved a series of preparation steps before any data could be taken. A sample first had to be mounted to the aluminum frame, which itself was mounted to the cold finger of the cryostat. Care was taken not to induce any strain on the sample at this step, which could produce misleading results. Following this, beam alignment was performed using the reflected light of the laser. The photoluminescence light given off by the sample's front surface would be radiated radially in all directions in a solid angle of 2π, centered on the spot being excited by the laser. The monochromator needed to be aligned along the path of these rays, so the incident light of the laser reflecting from the sample's surface was used for this alignment. This was performed prior to sealing the cryostat in order to avoid mistaking light reflected from the container window for light reflected from the sample's surface. The reflected light was focused onto the monochromator's slit, which was narrowed until a diffraction pattern could be seen. When this was achieved, the incoming signal alignment was complete. The cryostat could then be sealed and pumped by a mechanical pump for some 20-30 minutes to achieve the low pressure limit that the pump could provide. Cooling was initiated at this point by starting the compressor, which would bring the sample cold head down to a range of 10°K. Sample temperature was monitored by the temperature controlling electronics associated with the heater element. After reaching the low temperature limit, the room lights were switched off when the photomultiplier tube was in use to avoid overloading the tube from stray light signals. The software program was started on the desktop computer, and the monochromator reading on the mechanical dial was entered for reference. Scan speed and the wavelengths to be scanned were input as well, using a large span and fast speed for an initial scan to be performed on a sample with an unknown spectrum. Adjustments were made to the lock-in amplifier at this point, in order to fine

tune the angular setting for maximum signal and adjust the time constant for minimum signal fluctuation. Laser spot size was then controlled to produce as small a spot as possible to avoid any light scattering from the sample frame and to minimize the variation in signal due to film nonuniformities at the sample edges. With all adjustments made, a quick scan was necessary when using a new sample. A broad range for wavelength selection was made for this scan to give a general idea of where the luminescence signals were to be expected and how large the signals were going to be. Detector alignment could now be performed by slightly shifting its position to obtain a maximum signal by reading the lock-in output. This step was only utilized when a new sample was introduced, since moving the light detector during a series of scans on one sample would produce unwanted variations in peak amplitudes. The amplitude of the strongest signal was used as a guide for setting the lock-in amplifier's scale to try to obtain as close to the full scale position as possible for the strongest signal. After this was performed, an actual sample scan could now be run. The region of interest was keyed into the scan program using a relatively slow scan speed, and output was directed to the pen plotter for a permanent record.

When a temperature dependency was needed, a sample was scanned at low temperature initially. Its temperature was raised using the heater element and monitored by the silicon diode thermometer which provided output to the temperature controller. The sample's temperature was brought up in successive stages by allowing the temperature to stabilize at each temperature setpoint.

The only difference in the study of the GaSb sample was in the type of detector used. The PbS detector operated at room temperature, since it was not designed for use in a cooling chamber. It also showed a measurable delay in response to an input signal, which was to be expected for this crystal. Therefore, the chopper frequency was set to a lower value and the lock-in amplifier needed to be set to a longer time constant, which caused a reduction in resolution.

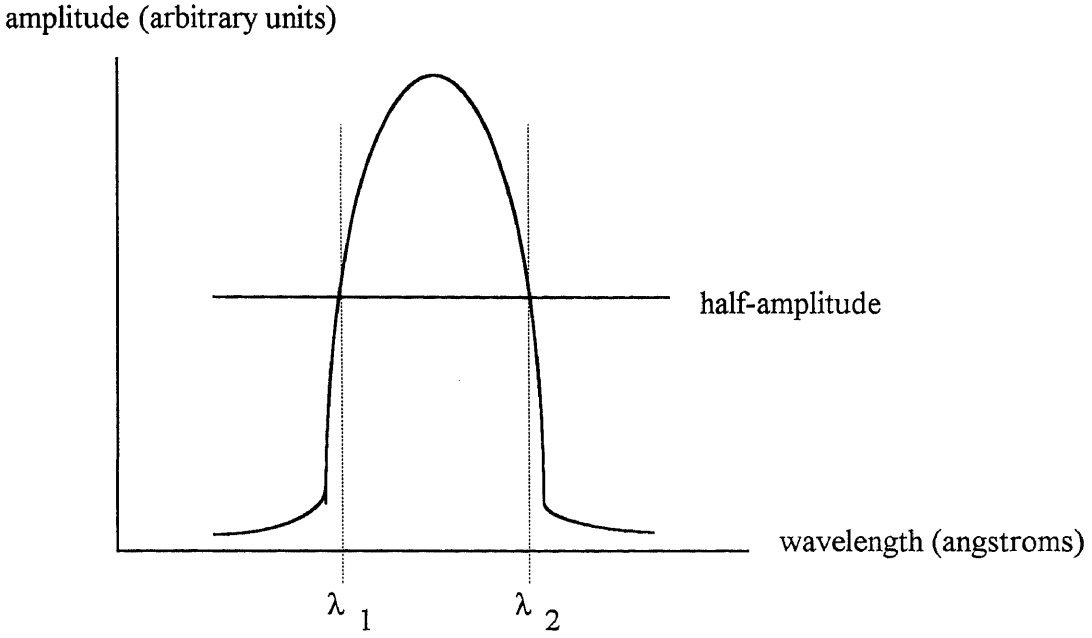

Figure 4.1 Full-width at half-maximum determination for emission peaks. The resulting wavelength values were converted to energy values, whose difference yields the FWHM of the emission peak.

4.3 Spectra Analysis

4.3.1 General considerations

Analysis of emission peaks began by calculating the wavelength positions each peak occupied on the scan plots. The plot scale was determined by multiplying the plotter speed, which was set at 100 angstroms per inch for all experiments, by the scan rate for the monochromator, which was supplied by the user to the interface software. Some of the wavelength markings are seen for the first few divisions on the sample plots included. Once a scale had been established, the peak positions were determined along with their widths.

An important characteristic for a spectral peak is the value of its full-width at half-maximum. The calculation of this parameter involves determination of the peak's half-maximum point on the y-axis, and using this value to find the two points on the x-axis which give the wavelength region for this portion of the peak. The difference in these

values provides a value for the FWHM, which is an important characteristic for the analysis to be performed upon it. This procedure is illustrated on the previous page as Figure 4.1. All wavelength data was converted to energy values using the relation

$$E\ (eV) = 1.24/\lambda\ (\mu m).$$

One last point to be made concerning the experimental procedure is that no intensity calibration was performed. If photoluminescence peak intensities are to be compared, some calibration must be performed for the equipment. The reason is due to a wavelength dependency of the monochromator grating efficiency, and especially the detectivity of the detector. Intensity calibration is usually performed by using a source with a known spectral shape, such as a blackbody source. A scan over the source will provide a spectrum which shows the type of corrections which are necessary if normalized data is to be taken. In this way, the wavelength dependency which all the equipment possesses will be removed.

For this study, the photomultiplier tube together with the monochromator grating and optics were assumed to have a relatively flat spectral dependency. This assumption was based upon information provided by the manufacturers of the equipment used. The setup for the GaSb sample involved the use of the PbS crystal detector, which does not have such a flat response. For the longer wavelengths scanned, it was also uncertain if the other components would have a wavelength dependency. This fact was kept in mind when analyzing the data, but such a consideration was not a problem. The peaks to be analyzed showed up within a relatively small wavelength span, and the relative intensities of the peaks varied to such a degree that adjustment of their heights was not necessary to interpret the data correctly. Calibration of equipment as just described would only be crucial for a comparison to spectra taken in another laboratory or for a comparison of peaks within one spectral plot. This second type of analysis would consist of measuring the height of two transition peaks close in amplitude but far apart in wavelength for emission efficiency comparisons.

4.3.2 Spectrum 1 - GaAs at 10°K

A scan of GaAs formed on GaAs bulk taken at 10°K from 6000 to 9000 angstroms is shown as Figure 4.1. A total of four peaks can be resolved for the region of interest from 8000 to 9000 angstroms. The energy gap of GaAs, from Blakemore's data (1982), is calculated at 1.519 eV for 10°K (representing no change in its value at 0°K).

The first peak was calculated at 1.503 eV, with a FWHM of 6 meV. This represents a transition having a reduction of only 16 meV from the bandgap value, so one or several BE states was suspected to cause this peak. Knowing this, an attempt was made to fit the high energy peak at 1.503 eV to some carefully conducted studies which have established values for bound exciton peaks in undoped GaAs samples. Work by Ashen (1975) has established a number BE peaks identified in various GaAs samples. The average position of all BE peaks due to seven identified impurities within their samples gives a value of 1.512 eV. Two other works have shown a BE found at 1.514 eV (Stringfellow and Linnebach 1979, 2213) and at 1.5142 eV (Swaminathan, *et al.* 1985, 5351) for undoped GaAs grown by MOCVD. Using a value of 1.514 eV based upon the more recent studies, the first peak position for this sample was adjusted to fit the established data. Based upon this fit, it was found that the spectrum taken for this sample needed to be shifted by -61 angstroms due to the 11 meV difference for this peak. This shift may have taken place due to possible misalignment within the monochromator as described in Section 3.4.2. The correction was assumed to be necessary for all data to be analyzed later, so only corrected values will be given from this point.

The width of the line here was typical of relatively pure GaAs bulk samples (Leite and DiGiovanni 1966, 841) and for undoped MOCVD samples (String-fellow and Linnebach 1979, 2213 and Swaminathan, *et al.* 1985, 5351). The later study was able to identify a number of sharp exciton transitions due to different impurity states. The resolution

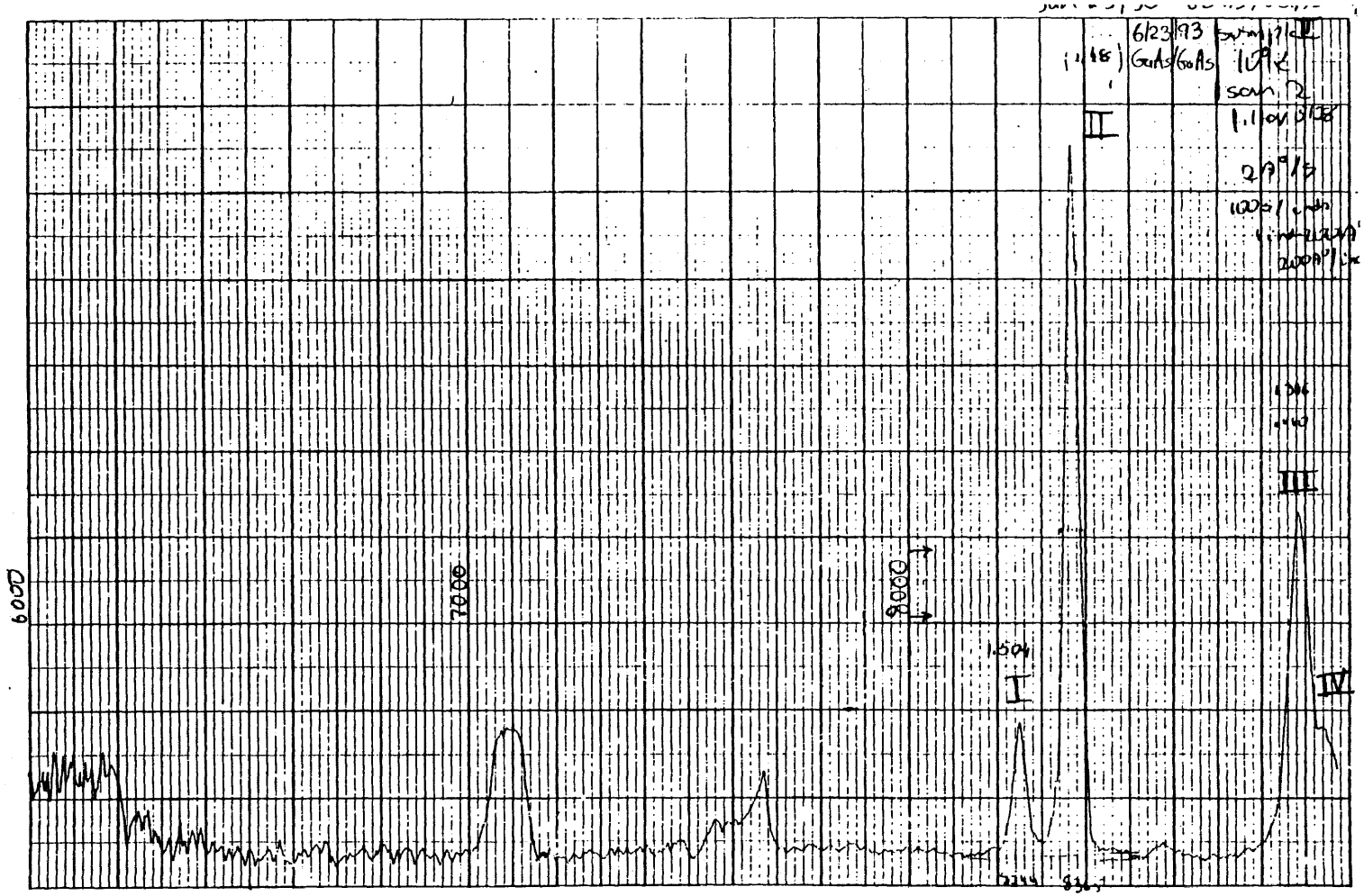

Figure 4.2 Photoluminescence spectrum of GaAs film on GaAs substrate taken at 10°K.

here did not permit this type of distinction, but it is assumed that a number of transitions took place in this region to cause a widening from the theoretical value of about .1 meV for a single bound exciton transition.

Having established the cause of the first peak, the second transition could be analyzed. It was found to take place at a value of 1.493 eV, and had a FWHM value of 6 meV. The narrow width of this transition places it as a probable FB peak. The peak represents a shift of 26 meV away from the bandgap, so an acceptor with such a binding energy was a likely cause. Consulting a list of GaAs sam-ples in which various impurities have been identified (Ashen, *et al.* 1975, 1051) shows that carbon acceptors have exactly this binding energy. An extensive study by Ashen, *et al.* (1975) has shown that carbon and zinc were two common impurities found in many VPE grown samples. Both of these contaminants may be possible for MOCVD processing as well, but the details of this particular MOCVD process were not well-known, so only a speculation could be made as to the possible impurities expected here. Carbon, in particular, is to be expected in high concentrations for many MOCVD samples (String-fellow 1978, 73), perhaps due to the trimethylgallium used $(CH_3)_3$). Consulting the table of values for binding energies due to acceptors in GaAs (Table 2.1), a number of shallow acceptors aside from carbon possess energies in the range seen here. Due to the expected high abundancy of carbon in processing along with its matching binding energy according to this source, carbon was assumed to be responsible for the FB transition seen in this sample. The narrow width of both peaks suggests a uniform distribution of impurities and a good crystal quality, free from a high concentration of gross defects.

A small hump at the low energy side of the FB peak (at 1.455 eV) may be a longitudinal optical phonon replica of the FB peak. Samples studied by Gilleo, Bailey, and Hill (1968) have shown that a duplication of several transitions with a separation distance of 37 meV can be attributed to the emission of a LO phonon associated with a given process.

Finally, a peak with a shoulder at low energy shows up at 1.405 eV and 1.397 eV, respectively. FB transitions were a likely cause, based upon the peak shapes and the fact that donors were not expected to be involved in these transitions, since no other DA transitions were seen. The acceptors causing the emissions seen here may be considerably deeper than the typical shallow acceptors found in GaAs. If one impurity is assumed to be responsible for each peak, then the impurities would have binding energies of 114 meV and 122 meV. Using Table 2.1, several deep acceptors are seen to lie in this region which may have been the cause for these transitions. Among these elements are silver (110 meV) and lead (120 meV). A more likely explanation for the set of peaks is that they may be due to defects within the sample which cause acceptor complexes to form. One laboratory group studying LPE GaAs detected a transition seen at 1.41 eV, which the study team had concluded was due to silicon impurity associated with an arsenic vacancy (Si_{As}-V_{As}) (Shin, *et al.* 1988, 737). In our case, since carbon was identified as an impurity, the 1.405 eV and 1.397 eV transitions may be ascribed to C_{As}-V_{As} complex centers. The control of both gallium and arsenic vacancies can be difficult in GaAs thin film formation, partially due to the high vapor pressure of arsenic which requires careful chemical flux control during growth (Swaminathan, et al. 1985, 5352).

4.3.3 Spectra 2 and 3 - AlGaAs at Low Temperature

Two different samples of $Al_xGa_{1-x}As$ were scanned, each having a different given ratio of Al to Ga. The first sample, with a given value of x = .25, produced a photoluminescence spectrum which appears as Figure 4.2. The plot which will be discussed at this point appears as the first scan in the figure, taken at 20°K. The second $Al_xGa_{1-x}As$ sample had a given value of x = .30, and its photoluminescence emission was measured at 11°K. The resulting plot is shown as Figure 4.3. The first sample produced three discernible peaks in the region from 7000 to 7400 angstroms. The second sample provided two resolved peaks in the region of 6000 to 6800 angstroms.

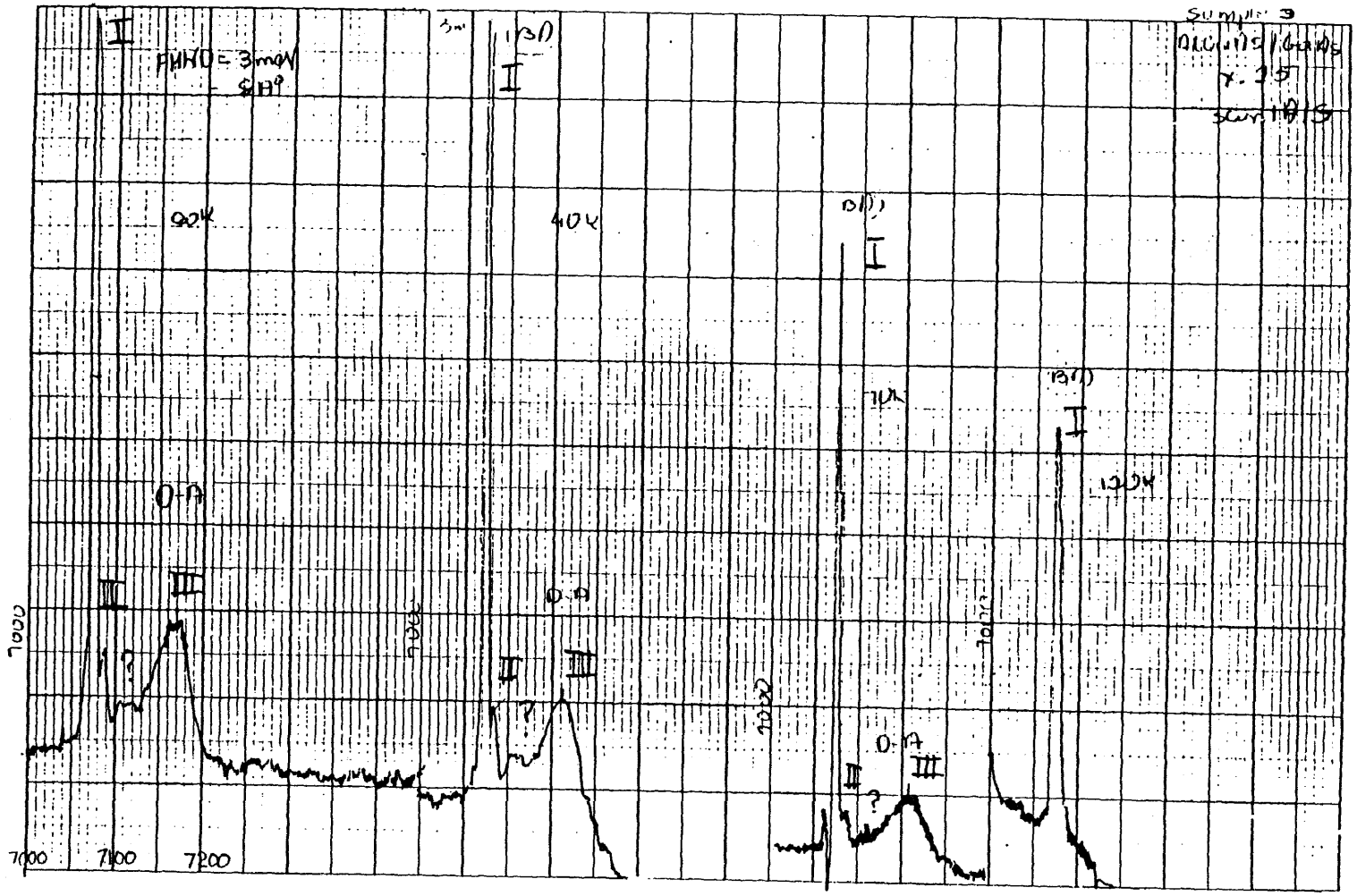

Figure 4.3 Photoluminescence spectra of $Al_{.25}Ga_{.75}As$ film on GaAs substrate taken at 20°K, 40°K, 70°K, and 120°K.

Examination of the high energy peak in both samples will provide a first clue as to the material quality and a give an accurate estimation for the true value of the aluminum percentage (x) in each. This statement can be made since a good quality film should produce one or several clearly identifiable bound exciton transitions which would appear at a point very near the bandgap energy, and the place where the BE transition takes place can be used to calculate x. The calculation of the Al/Ga ratio follows from the fact that the bandgap for the ternary compound increases with increasing aluminum content, shifting the position of the BE states linearly. The equation providing a calculation of the Al/Ga ratio is given as

$$x = \alpha(h\nu_{BE}(x) - h\nu_{BE}(0))$$

for $0<x<.35$, with $\alpha = .8032$ and $h\nu_{BE}(0) = 1.512$ eV (Dingle, Logan, and Arthur 1977, 210).

The first sample ($Al_{.25}Ga_{.75}As$) had a high energy peak at 1.768 eV with a FWHM of only 2 meV. Its narrow width almost positively identifies it as being due to an exciton recombination mechanism. Studies have been conducted which have shown that all high quality samples of AlGaAs grown by LPE (Dingle, Logan, and Arthur, 33a) and MOCVD (Stringfellow and Horn 1979, 794) will show strong BE and FB transition lines. Assuming a BE peak and using Dingle's formula gives a calculated value of x = .206 in this case. The second sample ($Al_{.30}Ga_{.70}As$) had its first peak at 1.988 eV and a larger FWHM value of 25 meV. Although this peak was considerably wider, it was assumed that sample quality was still good enough to provide for BE states. A calculation of Al percentage content gave an experimental value of x = .382 for the second sample.

The calculations which have been performed to determine Al content are only exact if the samples were scanned at a temperature very near absolute zero, so that the bandgap value does not change to a measurable extent. For the $Al_{.25}Ga_{.75}As$ sample taken at 10°K, the bandgap energy calculated to within 1 meV does not change. The $Al_{.30}Ga_{.75}As$ sample, taken at 20°K, will have a calculated change of only -1 meV.

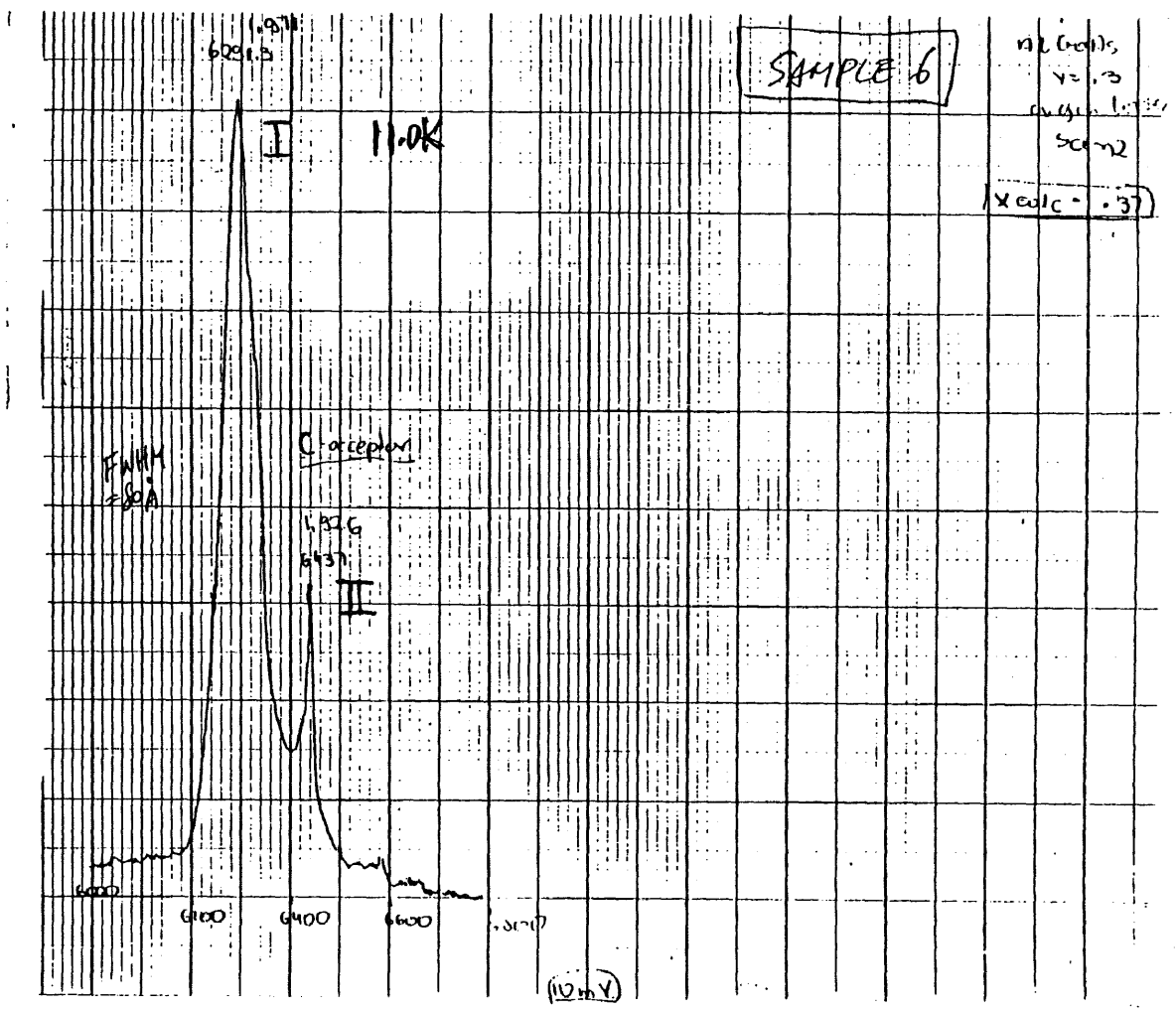

Figure 4.4 Photoluminescence spectrum of $Al_{.30}Ga_{.70}As$ film on GaAs substrate taken at 11°K.

Since the scan resolution was on the same order, no correction was necessary for this difference. Another point to be made is that the accuracy of the formula is in question for a value of x greater than .35, since the bandgap begins to show more of a quadratic behavior for higher aluminum content (Shur 1990, 626). No correction was made here, either, as the deviation in the calculated value of x from the maximum to be used was only .032 for the $Al_{.30}Ga_{.70}As$ sample, which is only a 9% increase above .35. In addition, Shur (1990) gives an energy gap dependency for AlGaAs based upon Al content in which the quadratic dependency is not to be used until $x \geq .45$.

A careful examination of the $Al_{.30}Ga_{.70}As$ scan shows that there may be several shoulders to the BE peak which contributed to its increased width, as compared to the first sample. The resolution of the scan did not permit a confirmation of the existence of several BE transitions, but it was assumed that several were taking place, based upon the total width of the peak.

Comparing the two samples to other undoped LPE and MOCVD samples brings out some important features. An extensive study by Stringfellow and Linnebach (1979) of a number AlGaAs samples has shown that typical MOCVD grown films did not exhibit the sharpness of the BE peak seen in the $Al_{.25}Ga_{.75}As$ sample here. The $Al_{.30}Ga_{.70}As$ sample seemed to be more typical of the specimens under this previous study, since their BE peaks were about 20 meV wide for $x \geq .20$. The study had shown that it was common for AlGaAs samples to exhibit a widening of all peaks with increasing x. A common explanation for the increased peak widths is that variations in Al/Ga ratios across the sample will produce variations in the bandgap throughout the specimen. Their conclusion was that the widening was due to increased donor plus acceptor numbers with increasing x, but this is only a hypothesis which was based upon mobility measurements. Referring to the more common explanation, the sharpness of the BE peak in the $Al_{.25}Ga_{.75}As$ sample provides evidence that the Al/Ga ratio was tightly controlled, and also that the impurity levels and sample defects were at a minimum.

The $Al_{.30}Ga_{.70}As$ sample had only one other detectable peak, whose position was calculated at 1.944 eV with a FWHM value of 4 meV. This represents a shift of 44 meV down in energy from the ascribed BE peak, which is sufficient to rule out any other BE transition as the cause. It is more likely that some well-defined acceptor level was providing for an FB transition. Since acceptor energy levels can shift with changes in Al/Ga ratios, the identification of specific impurities becomes a difficult matter in comparison to analyzing GaAs spectra (String-fellow and Linnebach 1979, 2212). Some impurities which have been suggested to exist for VPE samples are carbon, silicon, zinc, germanium, and tin (Ashen, *et al.* 1975, 1041). Carbon in particular is suspected to be a major impurity for MOCVD processing of AlGaAs (Stringfellow 1978, 73), but proving that any particular impurity was the cause for an FB peak could not be achieved in this study. Any of the aforementioned impurities may have possessed a binding energy in this sample which would have matched the observed value of about 51 meV.

If the band gap edge is well-defined for a sample of AlGaAs, then the binding energy for an impurity causing an FB peak can be estimated. This can be done by adding the FB peak shift from the BE peak position (44 meV) to the energy value for the free exciton (estimated at 5 meV from Wright's studies (1966)) and to the estimated binding energy of the exciton to the impurity site (about 2 meV, using the values obtained for GaAs samples by Ashen, *et al.* (1975)). The important characteristic to notice is the small FWHM value of 4 meV, which signifies that a well-defined band gap exists for this sample, with an impurity concentration below that which would cause impurity band formation.

The $Al_{.25}Ga_{.75}As$ sample contained two more resolved peaks on the low energy side of the identified BE peak which will now be discussed. A sharp edge to the BE peak was calculated at 1.764 eV having a FWHM value of about 2 meV. Since this peak lies only 4 meV away from the BE peak and has a width of the same size, it was proposed that another BE state was the cause. The identification of separate bound exciton states has

been attempted (Stringfellow and Linnebach 1979, 2213) using theoretical values for binding energies donors and acceptors will possess for excitons (Heim and Hiesinger 1974, 461). The basis for this identification is guesswork unless more information is available for the sample, so it can only be said that two BE states were seen for this sample, each one having a well-defined energy value. A possible emission peak appears as a broad structure in the spectrum next to the small BE peak, at 1.758 eV with a FWHM of 6 meV. The small size of the peak and its position on the shoulder of the third emission peak make its identification difficult. Resolution was not high enough to be able to determine if this was a single peak or a group of transitions, so the origin of the peak could not be determined. The last peak seen for this sample was calculated to be at 1.745 eV with a FWHM of 10 meV. It possesses a broad shape that a dominant DA transition is expected to have (see Section 2.3.2.1), and the location of the transition is in the range expected for such a process.

A calculation can be performed to estimate the binding energy of the acceptor, similar to the one done on the $Al_{.30}Ga_{.70}As$ sample when its FB peak was analyzed. An adjustment to account for the additional lowering of DA transitions from FB transitions due to the position of the donor within the bandgap (estimated to be about 3 meV by Leite and DiGiovanni (1966)) is necessary, as well as an adjustment to account for the Coulombic term in DA transitions (see Section 2.5.3.2). The Coulombic term could not be known for this calculation, but its existence implies that the actual binding energy may be lower by some amount since the term will increase the energy of the DA emissions. Performing the calculation with these two considerations in mind gives an upper limit for binding energy of about 33 meV for the shallow acceptor involved, assuming that this peak is a DA transition. Since the behavior of acceptors incorporated into AlGaAs

samples is not well known, and the true value of the binding energy of this peak was not known, the identity of the acceptor causing the transition could not be made. In GaAs samples, a number of shallow acceptors can fall into or just below this value (see Table 2.1).

4.3.4 AlGaAs Temperature Dependency

Figure 4.3 represents a set of four scans of the $Al_{.25}Ga_{.75}As$ sample taken at 20°K, 40°K, 70°K, and 120°K to examine its temperature dependency. A total of three peaks may be discerned for each scan, with the disappearance of all but one when the sample temperature was raised to 120°K.

Calculations of all peak positions show that there is no absolute shift in energy for any of the peaks beyond experimental resolution. In the case of GaAs, a bandgap shrinkage will take place which would shift all band-edge transitions. Using the temperature range of 20°K to 120°K, a GaAs sample would show a shift of 23 meV for these transitions. Since the high energy peak for the AlGaAs sample was determined to be a BE transition (Section 4.3.3), it would be a good indicator for measuring any band gap changes. Since no change was seen for this peak, the conclusion which can be made is that this sample exhibited no band gap change within experimental resolution for the temperature range of 20°K to 120°K. However, no reference could be found which provided any temperature dependency for AlGaAs, so this could not be confirmed.

The existence of the BE peak up to 120°K indicates a high exciton thermal stability for the sample as compared to GaAs samples prepared by the same laboratory, using the same process. The BE transition peaks for the GaAs samples tested had virtually disappeared at a temperature of only 45°K, by comparison. The two other resolved peaks on the low energy side of the BE peak can be seen up to a temperature of 70°K, although there is an expected reduction in amplitude.

The disappearance of the third and fourth peaks (at 1.758 eV and 1.745 eV, respectively) with temperature show what is expected to take place for DA transitions. As the sample temperature is raised, the shallow donors are ionized and the intensity of the peak will decrease. Typically, the DA transition becomes FB with increasing temperature, but no FB transition was determined to exist for this set of scans. It may be possible that FB transitions are taking place within the high energy peak at 1.768 eV, which was ascribed to be due to only exciton transitions because of its narrow width (2 meV). Since this peak's width did not change considerably at higher temperatures, the assignment of FB transitions to this peak region could not be done with confidence.

4.3.5 Spectrum 4 - GaSb at 10°K

The final spectrum for analysis is one of a GaSb sample taken across the IR region of 1.54 μm to 1.59 μm, as is displayed as Figure 4.4. A different monochromator grating was used in this case which had only one-fourth the line density of the other grating used. Because of this, the correction applied to shift spectra peaks was modified by multiplying it by four to give a resultant shift of -240 angstroms. Using this correction factor, a single strong peak was seen at 804.5 meV with a FWHM value of 3.5 meV. A small shoulder to this peak appears at 799.5 meV having a FWHM value of about 3.0 meV. The expected impurities and resulting transitions for this semiconductor are less well-known since it has not been studied to the same degree as GaAs and AlGaAs samples, but a similar analysis may be applied for this case which was used for other samples.

The spectrum exhibited here will be compared to one produced using an undoped LPE grown sample in a recent study (Wu and Chen 1993, 8497). A temperature dependence was examined in this separate study, which could not be performed here due to equipment failure. The energy values to be given for the work by Wu and Chen are those for the 19°K photoluminescence scans, as their sample's peak positions were seen to change with temperature. According to Wu and Chen, their sample's highest energy peak

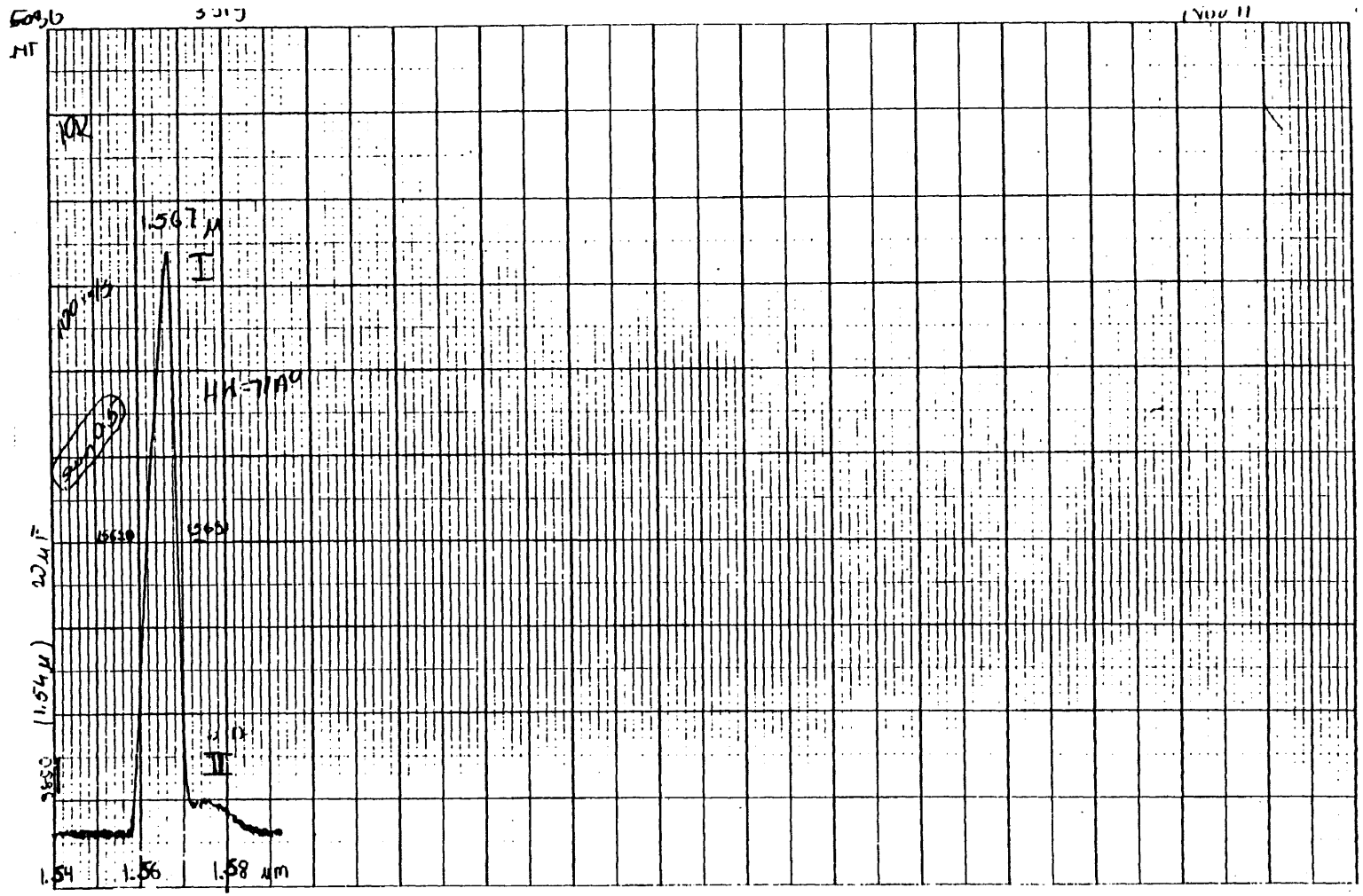

Figure 4.5 Photoluminescence spectrum of GaSb film on GaSb substrate taken at 10°K.

was a doublet, due to excitons bound to donors (at 808.2 meV) and excitons bound to a neutral acceptor (at 802.9 meV). Their second peak was said to be due to residual acceptors (at 777.8 meV), with its rounded shape said to be strongly suggestive of DA recombination. The term residual acceptor refers to an acceptor site due to a specific type of crystal defect which has been proposed to be common for this semiconductor (Allegre and Averous 1979, 379). Resolution was not good enough to determine if the high energy peak for the sample used in this study was due to more than one transition, and the small scale of the second peak for this sample makes any analysis difficult, but the low temperature employed together with the peak's shape make DA recombination a strong possibility. If a BE transition were assumed for the first peak in our sample, then using the corrected value of 804.5 meV places it only 3.7 meV away from the value calculated by Wu and Chen. The width of the peak seen in our sample agrees with the approximate value obtained of 5 meV for their BE peak.

The spectrum taken in this study at 11°K differed from Wu and Chen's taken at 19°K in two important aspects. The first of these differences is the small peak amplitude of DA transitions as compared to the BE peak amplitude in the sample studied in this laboratory. The BE to DA peak amplitude ratio for our sample was determined to be about 14:1. The second difference is the close distance of the BE peak to the DA peak in this sample. The lower temperature spectrum Wu and Chen obtained showed a higher DA peak amplitude relative to BE peak amplitude (about 4.5:1) and a greater separation distance for the BE peak to DA peak. The conclusion is that the sample studied in this laboratory showed exceptional crystal quality and impurity uniformity, as evidenced by the narrow, dominant BE peak. Wu and Chen's sample provided for BE/DA peak separation distance of 30.4 meV, while the difference seen for our sample was only 5 meV. It is therefore possible that the donor and acceptor levels seen in our sample may not be typical of those in LPE grown samples. The DA recombination seen for this sample may have been due to much shallower acceptors than those seen in some LPE samples.

CHAPTER 5

CONCLUSIONS

A summary of experimental findings will be provided to clarify the important results. Four epitaxial layer MOCVD grown films were studied by examining low temperature photo-luminescence emissions. The samples used in this study consisted of GaAs film on GaAs bulk, $Al_{.25}Ga_{.75}As$ on GaAs bulk, $Al_{.30}Ga_{.70}As$ on GaAs bulk, and GaSb on GaSb bulk. The GaAs sample provided an FB peak which allowed for the finding of an acceptor with a binding energy of 26 meV, which was assumed to be carbon. The $Al_{.25}Ga_{.75}As$ sample had shown a narrow BE transition which was stable up to a temperature of 120°K. Analaysis of the spectra led to the conclusion that sample had a low impurity content and a well-controlled ratio of Al to Ga throughout the film. The experimental value of the Al/Ga ratio was found to be x=.206. This sample also appeared to possess an acceptor level whose binding energy was determined to be no greater than 33 meV. In addition, no temperature dependency was seen to exist for emisssion in the range of 20°K to 120°K. The $Al_{.30}Ga_{.70}As$ sample exhibited a resolved BE peak which was not as narrow as the $Al_{.25}Ga_{.75}As$ sample, but typical of other MOCVD AlGaAs. The experimental Al ratio content for this sample was found to be x=.382. An FB peak provided for the clue to the existence of an acceptor whose binding energy was calculated at 51 meV. Lastly, the GaSb sample had shown a strong, narrow BE peak which identified the film to be of good crystal quality. Comparison made to undoped LPE samples grown in another laboratory provided evidence for this conclusion. The ascribed DA transitions within this sample's spectrum led to the possibility of the existence of shallow donor levels whose binding energy was much less than the acceptor levels seen the LPE samples.

REFERENCES

Allegre, J. and M. Averous 1979. *American Institute of Physics Conference Series.* 46: 379.

Blakemore, S. 1982. "Semiconductor and Other Major Properties of GaAs." *J. Appl. Phys.* 53,10: 123-181.

Ashen, D. J., P. J. Dean, D. T. J. Hurle, J. B. Mullin, A. M. White, and P. D. Greene 1975. "The Incorporation and Characterization of Acceptors in Epitaxial GaAs." *Phys. Chem. Solids.* 36: 1041-1053.

Bernussi, A. A., C. L. Barreto, M. M. G. Carvalho, and P. Motisuke 1988. "Photoluminescence of GaAs Films Grown by Vacuum Chemical Epitaxy." J. Appl. Phys. 3,64: 1358-1362.

Casella, R. C. 1963. *J. Appl. Phys.* 34: 1703.

Dingle, R., R. A. Logan, and J. R. Arthur Jr. 1977. *Inst. Phys. Conf.* 33a: 210.

Elliot, R. J. 1957. *Phys. Rev.* 108: 1384.

Gilleo, M. A., P. T. Bailey, and D. E. Hill 1968. "Free-Carrier and Exciton Recombination Radiation in GaAs." *Physical Review.* 174,3: 898-905.

Grahn, M. T., M. Schneider, W. W. Ruhle, K. von Klitzing, and K. Ploog 1990. *Phys. Rev. Lett.* 64: 2426.

Heim, U. and P. Hiesinger 1974. *Phys. Status Solidi.* 66: 461.

Jain, J. K. and S. Das Sarma 1989. *Phys. Rev. Lett.* 62: 2305.

Kastalsky, A., V. J. Goldman, and J. Abeles 1991. *Appl. Phys. Lett.* 21,59: 2636-2638.

Kittel, C. 1986. Introduction to Solid State Physics. Sixth Edition. New York: John Wiley and Sons, Inc.

Kudo, K., Y. Makita, I. Takayasu, T. Nomura, T. Kobayashi, T. Izumi, and T. Matsumori 1985. "Photoluminescence Spectra of Undoped GaAs Grown by Molecular-Beam Epitaxy at Very High and Low Substrate Temperatures." *J. Appl. Phys.* 59,3: 888-891.

REFERENCES
(Continued)

Lee, M., D. J. Nicholas, K. E. Singer, and B. Hamilton 1985. "A Photoluminescence and Hall-Effect Study of GaSb Grown by Molecular Beam Epitaxy." *J. Appl. Phys.* 8,59: 2895-2900.

Leite, R. C. C. and A. E. DiGiovanni 1966. "Frequency Shift with Temperature as Evidence for Donor-Acceptor Pair Recombination in Relatively Pure n-Type GaAs." *Physical Review.* 153,3: 841-843.

Mahan, G. D. 1967. *Phys. Rev.* 153: 882.

Milnes, A. G. 1973. Deep Impurities in Semiconductors. New York: Wiley.

Pankove, J. 1971. Optical Processes in Semiconductors. New York: Dover Publications, Inc.

Reynolds, D. C., K. K. Bajaj, C. W. Litton, G. Peters, P. W. Yu, R. Fischer, D. Huang, and H. Morkoc 1986. "Lifetimes, Ionizations Energies, and Discussion of the Emission Lines in the 1.5040-1.5110 eV Range in GaAs." *J. Appl. Phys.* 7,60: 2511-2516.

Ridley, B. K. 1989. *Phys. Rev.* B39: 5282.

Schairer, W. and E. Grobe 1970. *Sol. State Comm.* 8: 2017.

Shin, K. C., M. H. Kwark, M. H. Choi, M. H. Oh, and Y. B. Tak 1988. "Photoluminescence Investigation of the 1.356 eV Band and Stoichiometry in Undoped GaAs." *J. Appl. Phys.* 65,2: 736-741.

Shur, M. 1990. Physics of Semiconductor Devices. N. Holonyak, Jr. Englewood Cliffs: Prentice Hall.

Stringfellow, G. B. 1978. *Ann. Rev. Mater. Sci.* 8: 73.

Stringfellow, G. B. and G. Horn 1979. *Appl. Phys. Lett.* 34: 794.

Stringfellow, G. B. and R. Linnebach 1979. "Photoluminescence of Shallow Acceptors in Epitaxial $Al_xGa_{1-x}As$." *J. Appl. Phys.* 51,4: 2212-2217.

Streetman, B. 1990. Solid State Electronic Devices. N. Holonyak, Jr. Englewood Cliffs: Prentice Hall.

REFERENCES
(Continued)

Sturge, M. D. 1962. *Phys. Rev.* 127: 768.

Swaminathan, V., D. L. Van Haren, J. L. Zilko, P. Y. Lu, and N. E. Schumaker 1985. "Characterization of GaAs Films Grown by Metalorganic Chemical Vapor Deposition." *J. Appl. Phys.* 12,57: 5349-5353.

Tatham, M. C., J. F. Ryan, and C. T. Foxon 1989. *Phys. Rev. Lett.* 63: 1637.

Thomas, D. G., M. Gershenzon, and F. A. Trumbore 1964. *Phys. Rev.* 133: A269.

Wicks, G., W. I. Wang, C. E. C. Wood, L. F. Eastman, and L. Rathbun 1981. "Photoluminescence of $Al_xGa_{1-x}As$ Grown by Molecular Beam Epitaxy." *J. Appl. Phys.* 52,9: 5792-5796.

Wright, G. B. 1966. "International Conference on Luminescence, Budapest." N.p.: n.p.

Wu, M. and C. Chen 1993. "Photoluminescence of Liquid-Phase Epitaxial Te-Doped GaSb." *J. Appl. Phys.* 12,73: 8495-8501.

Yariv, A. 1975. Quantum Electronics. New York: Wiley.